Preparation of Fine Spinel and Cordierite Ceramic Powders by Mechano-chemical Techniques

By

Emre YALAMAÇ

**A Dissertation Submitted to the
Graduate School in Partial Fulfillment of the
Requirements for the Degree of**

MASTER OF SCIENCE

**Department : Materials Science and Engineering
Major : Materials Science and Engineering**

**İzmir Institute of Technology
İzmir, Turkey**

July, 2004

We approve the thesis of **Emre YALAMAÇ**

Date of Signature

---------- **27.07.2004**

Assoc. Prof. Dr. Sedat AKKURT
Supervisor
Department of Mechanical Engineering

---------- **27.07.2004**

Assoc. Prof. Dr. Metin TANOĞLU
Department of Mechanical Engineering

---------- **27.07.2004**

Asst. Prof. Dr. Fehime ÖZKAN
Department of Chemical Engineering

---------- **27.07.2004**

Prof. Dr. Muhsin ÇİFTÇİOĞLU
Head of Interdisciplinary
Materials Science and Engineering Program

ACKNOWLEDGEMENTS

I would like to express my sincere gratitude to my advisor, Assoc. Prc Sedat AKKURT for his supervision, guidance and encouragement throughout this study.

I am also grateful to IYTE-CMR staff for their help and technical support.

Special thanks to Umut Başak BALIKLI for her help, support, encouragement and understanding.

I would like to appreciate deeply to Mücahit SÜTÇÜ, Yelda ERGÜN and all my friends for their friendship, support and understanding.

Finally, I would like to thank my parents “Sevim YALAMAÇ and Ahmet YALAMAÇ” and my brother and sister for their support and encouragement.

ABSTRACT

Low temperature synthesis of cordierite and magnesium aluminate spinel powders has been attracting attention in recent years due to new potential applications. The use of mechanochemical methods to achieve partial or complete structural disorder as a tool to lower the sintering temperatures has also been increasingly reported.

In this study, spinel was produced by intense milling of a mixture of $Mg(OH)_2$ and $Al(OH)_3$. Detailed phase characterization of the synthesized loose powder spinel was performed using XRD and DTA. SEM was used for the analysis of ground powder morphology and particle size. Amorphization was observed after 50 minutes of grinding at 600 rpm. 110 minutes of grinding led to partial growth of spinel. Temperatures less than 1000^oC were able to produce spinel powders.

In the second part of the study, cordierite was synthesized by mixing proper amounts of various combinations of alumina or $Al(OH)_3$ (as a source of Al_2O_3), kaolin (as a source of SiO_2 and Al_2O_3), and talc (as a source of MgO and SiO_2). Detailed microstructural characterization of the synthesized pellets was performed by using SEM. Other techniques used for analysis of powder products were XRD, DTA and FTIR. One of the four possible mixture combinations was processed by using mechanochemical synthesis. This technique was analyzed by the use of statistical experimental design (SED) in order to understand the effects of process variables on the amount of synthesized product. Temperature was the most important factor and grinding speed-grinding time interaction was the next significant variable. These results were expected because lower grinding speed and longer grinding time generates a similar amount of grinding action compared to higher speeds and lower times. The cordierite mixture was completely amorphized by grinding at 300 rpm for 60 minutes based on XRD peak intensity measurements. Temperatures as low as 1150^oC were able to produce cordierite ceramic.

In addition to the mechanochemical technique, the effect of additive use and the combined effect of additive use and grinding on cordierite synthesis were also studied. These factors further decreased the synthesis temperature down to about 1050^oC.

ÖZ

Son yıllarda, kordiyerit ve magnezyum alüminat spinel tozlarının düşük sıcaklıkta sentezlenmesi potansiyel uygulama alanlarından dolayı ilgi uyandırmaktadır. Kısmen ya da tamamen yapısal düzensizliğe ulaşmak için mekanokimyasal yöntemlerin sinterleme sıcaklıklarını düşüren bir araç olarak kullanımı artarak bildirilmektedir.

Bu çalışmada, $Mg(OH)_2$ ve $Al(OH)_3$ karışımının yoğun öğütülmesi ile spinel üretilmiştir. Sentezlenen spinel tozlarının ayrıntılı faz karakterizasyonu X-Işını Kırınımı (XRD) ve Diferansiyel Sıcaklık Analizörü (DTA) kullanılarak yapılmıştır. Öğütülen tozun morfolojisi ve tane boyutu analizi için taramalı elektron mikroskobu (SEM) kullanılmıştır. 600 rpm ve 50 dakika öğütme sonunda amorf yapı gözlenmiştir. 110 dakika öğütme kısmi spinel oluşumuna yol açmıştır. 1000^oC'nin altındaki sıcaklıklarda spinel tozu sentezlenmiştir.

Çalışmanın bir sonraki kısmında, alümina veya $Al(OH)_3$ (Al_2O_3 kaynağı olarak), kaolen (SiO_2 ve Al_2O_3 kaynağı olarak), ve talk (MgO ve SiO_2 kaynağı olarak)'ın çeşitli kombinasyonlarının uygun miktarlarda karıştırılmasıyla kordiyerit sentezlenmiştir. Sentezlenen peletlerin ayrıntılı mikroyapısal karakterizasyonu SEM kullanılarak yapılmıştır. Toz ürünlerin analizleri için XRD, DTA ve FTIR kullanılmıştır. Karışım kombinasyonlarından biri mekanokimyasal sentezleme yolu ile çalışılmıştır. Bu teknik, proses değişkenlerinin sentezlenen ürün miktarı üzerine etkisinin anlaşılabilmesi için istatistiksel deney dizaynı (SED) kullanılarak incelenmiştir. SED'ye göre sıcaklık birinci ve öğütme hızı-öğütme süresi ilişkisi ise bir sonraki en önemli etkendir. Bulgular, düşük öğütme hızlarının daha uzun öğütme süresi gerektirdiği ve tam tersinin de geçerli olduğu genel bilgisi ile örtüşmektedir. Kordiyerit karışımı 300 rpm'de 60 dakika öğütülerek tamamen amorf hale gelmiştir ve bu öğütme kombinasyonu en iyi XRD sonucunu vermiştir. 1150^oC'ye kadar olan sıcaklıklarda kordiyerit seramiği üretilebilmiştir.

Mekanokimyasal tekniğe ek olarak, kordiyerit sentezi üzerine katkı kullanımı ve katkı kullanımı ile öğütmenin birlikte etkileri çalışılmıştır. Bu faktörler sentezleme sıcaklığını biraz daha düşürerek 1050^oC seviyesine indirmiştir.

TABLE OF CONTENTS

LIST OF FIGURES

LIST OF TABLES

CHAPTER 1

INTRODUCTION

Cordierite ($2MgO.2Al_2O_3.5SiO_2$) is an important ceramic material due to its low thermal expansion coefficient ($0.7*10^{-6}$ K^{-1}, 25-1000^oC) and low dielectric permittivity ($\varepsilon r \approx 4$ at 1 MHz). It is used in many industrial applications, for example, ceramic kiln furniture and ceramic honeycomb substrates in automotive exhaust systems in which the low thermal expansion and/or the resistance to the thermal shock is important and substrates in the microelectronic applications because of its low dielectric permittivity. Cordierite is used in many areas but natural cordierite is extremely rare and seldom occurs in commercial quantities. All cordierite produced are, therefore, from synthetic origin.

Magnesium aluminate spinel ($MgO.Al_2O_3$) is widely used in ceramic industry because it provides a combination of desirable physical, chemical and thermal properties, both at normal and elevated temperatures. It is used in refractories industry due to its high resistance to attack by most of the acids and alkalis. In addition, it is very useful in the electrical, energy and optical technologies. It has radiation resistance with good insulating properties. Spinel is to be applied to dielectric windows of fusion reactors or electrical insulators in radiation environments [1].

Cordierite and magnesium aluminate spinel ceramic materials have been investigated by many scientists. A wide range of synthesis methods have been proposed in order to decrease the synthesis temperature and increase the physical properties of these ceramics. Production methods such as, co-precipitation, sol-gel, slip casting have some advantages and disadvantages when compared to each other. In this study, mechanochemical techniques were used to decrease the synthesis temperature of these ceramics.

Mechanochemistry is a branch of science dealing with chemical reactions of solids, which take place under mechanical activation. It is the subject of increasing interest in relation to solid state science and technology. Mechanochemical procedures have great advantages compared to traditional technological methods. For example, they simplify the process by decreasing the number of technological stages and they are ecologically safe because they exclude the operations that involve the use of solvents.

Mechanochemical synthesis has great potential for novel powder synthesis at low temperature in addition to benefits derived from decreasing sintering temperatures and denser bodies. Intense grinding activates ceramic powders which enhances the development of solid-state processes. The mechanical energy produces structural imperfections in the powder particles during grinding and this effect increases the reactivity of ground materials. In addition, grinding which is based on impact and friction, increases the chemical reaction rates via particle size reduction, which increases the specific surface area [2].

Liquid phase sintering techniques are commonly used in electronic ceramics production. Many electronic ceramics may be co-fired with metals at reduced temperatures. During this process, oxide additives are used that accelerate the densification rate of ceramics as compared to the pure systems [3]. In addition to densification, these oxide additives decrease the sintering temperatures.

The objective of this study is to decrease the cordierite and spinel synthesis temperature via mechanochemical techniques. Another objective is to investigate the combined effect of additives and grinding on cordierite synthesis.

In the first part of the thesis, spinel was synthesized by using intense grinding. The $Mg(OH)_2$ and $Al(OH)_3$ powders were mixed and mechanically activated in planetary mono mill. After mechanical activation, the loose powders were heat treated at different temperatures.

In the second part of the study, cordierite synthesis was investigated. Laboratory powder synthesis tests were planned by the use of statistical experimental design (SED). The objective was to understand the effects of process variables on the amount of synthesized product. Full factorial experimental design was chosen in this study. The talc, kaolin, alumina and aluminum hydroxide were mechanically activated at different grinding speeds and grinding durations. After grinding, the powder mixtures were compacted and fired at different temperatures for different soak times.

In order to investigate the combined effect of additive use and grinding, magnesium borate ($2MgO.B_2O_3$) was synthesized to use as an additive. Synthesized magnesium borate was added into the cordierite mixture with different percentages (2 and 5 wt%) and the effect of this additive on synthesis temperatures ranging from 1000 to 1300^oC for cordierite were investigated. In the next step, the combined effect of grinding and additive use was investigated in order to lower the synthesis temperature. XRD, DTA and FTIR were used for characterization of the phases. Morphology of

ground particles was observed by using SEM. Densities and porosities of all heated pellets were also measured in this study.

CHAPTER 2

MECHANOCHEMISTRY

The ceramic powder synthesis technique that is employed in this thesis is mechanochemical treatment of precursor powder particles followed by heating. In this chapter, mechanochemistry of solids is briefly presented.

2.1. Development of Mechanochemistry

Mechanochemistry, a branch of chemistry, is concerned with both the study of chemical reactions, which occur under the action of mechanical forces, and reactivity of mechanically shredded solids. The original aim of the application of mechanical energy on solids was their disintegration and the production of surface-rich powders [4].

The effect of mechanical stress on the course of chemical reactions is one of the earliest experiences of mankind. Mechanochemical effects have been utilized since prehistoric times, when primitive man used friction to make fire, and it is still frequently used in many fields of human activity. The utilization of the sensitivity of explosives toward shock and friction in traditional mining and in military techniques are well-known examples.

Early experimental mechanochemistry was mentioned by Theophrastus of Eresus in his book *De Lapidibus* (*On Stones*) published at the end of the fourth century B.C. where he described the mechanochemical preparation of mercury from cinnabar. According to Takacs, examples of other mechanochemical reactions documented between 300 B.C. and the end of 1800s are mentioned in Agricola's *De natura Fossilicum*. However, the majority of review articles refer to experimental works of Carey Lea who described the decomposition of silver and mercury during attrition in a mortar and F. W. Ostwald who focused on theoretical relationship between chemical and mechanical energy.

In the beginning of the 20th century, Flavitsky and Parker studied the reactions that took place under mechanical treatment of solid mixtures. Their articles were pioneer works for improved understanding of the mechanism of solid-state reactions.

Solid-state mechanochemistry has developed alongside solid-state chemistry in this century.

In 1920s mechanochemistry was applied in the pulp and paper industry. Grinding provided a beneficial effect on the cellulose solubility by the mechanical destruction of the macromolecule and creation of new hydrophilic groups in the place of disrupted valence bonds.

In the early 1940s, effect of mechanochemistry on the inorganic solids was experimentally described. The experiments showed that mechanically induced phase transformation took place in minerals during milling. In a review presented on the 1st European Symposium on Comminution, Peters stated that all kinds of solid-state reactions can be observed during milling, beginning with simple decomposition reactions and ending with complicated syntheses from multicompartmental systems [5].

By the end of 1960s, oxide-dispersion strengthened (ODS) nickel- and iron-base superalloys were produced by ball milling, called "mechanical alloying", for applications in the aerospace industry. Mechanical alloying (MA) is also a dry (solid-state) powder processing technique like mechanochemical processing (MCP). Although the general principles and mills for operation are similar in both techniques, the main difference between the two techniques is that while a chemical reaction occurs in (MCP), such reaction need not occur in MA [6].

2.2. Mechanical Action on the Chemical Properties of Solids

Mechanical action takes place on a solid usually by combination of pressure and shear. In addition to hydrostatic loading, which is the most widely investigated technique, the effect of shear forces on chemical reactions of solids are presented. The devices usually used for this purpose are grinding mills.

There are three main types of devices:

a) The mills of shock action: fluid energy or jet mills, turbulent mills and high peripheral-speed pin mills. In these devices mechanical action is produced as a result of the collision of a particle, accelerated to high speed in gas jet, with a target (jet mills), or conversely, as a result of the collision of the moving solid blade with the particles (high peripheral-speed pin mills—disintegrators).

b) The devices of shear action, rollers, Leche mills. Here, mechanical action is produced by a shift when one solid surface moves across another, the substance under treatment being placed on the latter.
c) Various kinds of ball mills like planetary and vibration devices, Spex mills. These devices create pressure and shear during grinding and mechanical action occurs due to these forces. The relation between pressure and shear can be varied in a wide range, depending on construction features of a mill and its operation regime.

During grinding, mechanical action causes the appearance of strain field in a solid. The strain field takes place by the shifts of atoms from equilibrium stable positions, the changes of bond lengths and angles, and in some cases the excitation of electron subsystem. All these states are metastable so their formation is followed by relaxation via different channels. A well-studied and understood channel is the relaxation of the energy (accumulated in strain field) into heat. Another channel is plastic deformation. The accumulation of energy at this channel, in the case when there are sites in a crystal in which the strain is concentrated, can lead to the destruction of the crystal (crushing) and thus to the formation of a new surface. While crushing proceeds, the size of crystals decreases to some critical value. Further energy supply to these crystals of limiting size causes further deformation of crystals, energy accumulation in the volume or at the surface of crystals, and finally amorphization. In some cases, the defects are formed in order, and instead of amorphization, transition into a metastable polymorphous state occurs. Sometimes the relaxation of strain field results in the rupture of chemical bonds (mechanochemical reaction occurs). The four processes, namely, the accumulation of defects, amorphization, the formation of metastable polymorphous forms, and chemical reaction, are united by the term “mechanical activation.” [5].

2.3. Applications of Mechanochemistry

Applications of MA and MCP are not limited to scientific curiosity in synthesizing materials with non-equilibrium/metastable crystal structures and microstructures. Examples for industrial applications are briefly given below.

Mechanical milling has been used in mineral processing basically to increase the surface area and improve the chemical reactivity of the milled materials. However, the

development of research in mechanochemistry and mechanical activation of solids show that mechanical activation increases defect concentration and thus changes the reactivity of the solids in addition to reduction of particle size.

The process of mechanochemical leaching was patented and tested on a pilot-plant scale in Easten Slovakia. The mechanochemical treatment improved the degree of recovery and the rate of leaching of antimony. This process takes place at a lower temperature and for much shorter leaching times in comparison with the SUNSHINE process currently used in the United States.

Another application of mechanochemistry is synthesis of nanocrystalline materials. It has been utilized to produce nanosize pure metals, alloys and compounds at room temperature. Nanocrystalline ZrO_2 powder is produced by ball milling a mixture of zirconium chloride with MgO according to reaction:

$$ZrCl_4 + 2MgO \rightarrow ZrO_2 + 2MgCl_2$$

The reaction kinetics are substantially faster than in conventional methods. ZnS, CdS and Ce_2S_3 have been also synthesized by mechanochemical reaction.

Oxide-dispersion strengthened (ODS) alloys have been produced by mechanically alloying. Production of these alloys is difficult by methods like conventional ingot metallurgy (IM). They are mechanically strong both at room and elevated temperatures. The uniformly dispersed very fine (5-50 nm) oxide particles (commonly Y_2O_3 and ThO_2), which are stable at high temperatures, inhibit dislocation motion in the metal matrix and increase the resistance of the alloy to creep deformation.

In addition to real applications of mechanochemistry, some potential applications of MA materials are as follows. With increasing interest in “green” energy sources, relatively low-purity requirement hydrogen storage materials are the most promising for next MA applications [6]. According to some research [7-9], Mg-based hydrogen storage alloys could be produced by MA. The mechanically alloyed composite material (Mg + *x* wt.% YNi) exhibited higher hydrogenation kinetics than pure Mg at different hydrogenation temperatures.

Mechanochemical procedures belong to the environmentally friendly ones. The main advantages in comparison with the traditional technological procedures are:
(a) Decrease in the number of technological stages. Simplification of the process;

(b) ecological safety of the method, resulting from excluding the operations that involve the use of solvents, intermediate fusion, etc.; (c) the possibility of obtaining a product in the metastable state, which is difficult (or impossible) to obtain using traditional technological methods.

Mechanochemistry has also some problems, which are connected with use of devices and energy consumption. The main problem is the contamination of the material being milled by wear of the mill vessel and grinding media. In order to both protect the treated material from contamination and for purification of the ground products, different methods are proposed. The main method for elimination of unfavourable contamination is using same material for grinding reactor and media and ground material hardness has to be lower than grinding media and vessel.

Mills are usually used for mechanical activation. It is important to understand that the goals of mechanical activators and goals of mills are different. The major advantages of good mills are minimum energy consumption for the achievement of the maximum specific surface area. However, the main point for the good mechanical activator is the maximum energy transmitted by means of the activator into the chemical process or accumulated in the solid in form of defects, which will be used further in the chemical process. Because of this, a good mill does not always mean a good mechanical activator, and vice versa. This is the reason why the stages of reagent grinding, mixing, and performing the reaction, which are held together under the laboratory conditions, should be separated, while optimizing the process and preparing it for industrial application. These stages should be performed using different regimes [5].

CHAPTER 3

SYNTHESIS OF CORDIERITE AND SPINEL

In this chapter a literature review of the general characteristics of spinel and cordierite as well as their uses, properties and production methods are presented. In the first part, cordierite will be presented. Spinel will follow in the next section.

3.1. Cordierite

Cordierite was discovered by the French geologist Cordier in 1913. It has been the subject of extensive research since that time. Cordierite is the most unique ceramic material, because it has excellent thermal shock ($\Delta T>350$ K) resistance due to its low thermal expansion (as low as $0.7*10^{-6}$ K^{-1}, 25-1000^{o}C) [10]. Its published physical properties are given in Table 3.1.

Table 3.1. Main Physical Properties of Cordierite

$T_{melting}$ (^{o}C)	**Density** (g/cm^3)	**Crystal structure**	**Lattice constant** (Å)	**Refractive index**	**Molecular Weight** (mg)
1460	2.65	Orthorhombic	a = 17.13, b = 9.8, c = 9.35	1.55	584.95

Karkhanavala and Hummel, investigated the polymorphs of cordierite as far back as 1953. Their results indicated that three polymorphs exist, a stable low-temperature (β) form, a metastable low-temperature (μ) form, and a stable high-temperature (α) form. The high-temperature form can be obtained by solid-state reaction of batch material at 1300^{o}C to 1460^{o}C, or by crystallization of the glass between 1050^{o}C and 1460^{o}C. The metastable low-temperature form is not easily developed and requires many hours of crystallization of finely powdered glass at temperatures around 800^{o}C and 900^{o}C. The stable low-temperature form is developed

only by hydrothermal treatment of glass, the μ form, or the α form at temperatures below 830^{o}C [11].

Cordierite and cordierite-based-glass ceramics are promising materials as substrates in the microelectronic applications because of their low dielectric permittivity ($\varepsilon r \approx 4$ at 1 MHz). For example, they can be co-fired with copper at low temperature to form electronic substrates [12]. In addition, decreasing cordierite sintering temperature is also essential for circuit materials, since higher temperatures would cause the circuit materials to be oxidized. Therefore, various techniques such as slip casting [13], chemical precipitation [14] and solid powder reaction [15, 16] have been investigated in order to decrease the sintering temperature of cordierite. Cordierite and cordierite-based-glass ceramics also have a general use in thermal applications because of their low thermal expansion property, e.g. kiln furniture and substrates of catalyst for exhaust gas emissions control in automobiles [10].

Thermal shock resistance is one of the key requirements for ceramic honeycomb substrates coated with catalysts widely used for controlling automotive exhaust emissions. Cordierite combines relatively low thermal expansion (need for thermal shock resistance) with relatively high refractoriness (need for operating in severe exhaust environments at high temperatures). It is also inert to catalysts and the oxide coatings used as washcoats. Finally, it can be extruded into honeycomb substrates of suitable porosity and adequate mechanical strength [10].

Because cordierite is not found in nature in tonnage quantities, it must be synthetically produced using various techniques. These techniques are briefly presented in this section In the next section, mechanochemical cordierite synthesis studies are explained.

3.1.1. Cordierite Synthesis

As explained in section 3.1, cordierite is a significant ceramic material that needs to be produced in tonnage quantities. Its production has been the subject of extensive research. Techniques for cordierite synthesis include heating of solid-solid mixtures of talc, kaolinite, alumina, and aluminum hydroxide in addition to mechanochemical treatments.

A study by Awano *et.al.*, involved the use of grinding after sol-gel process. He suggested that mixed silica sol, boehmite sol, and magnesium nitrate solution for co-

precipitation and gelation of precursor-gel via an adjustment of solution pH. Grinding was done using a media-agitating type of mill. The agitator was maintained at 115 rpm for 24 hrs. As a result of their study, the ground powder crystallized from the amorphous and through the intermediate phases to a cordierite single phase at 1250^{o}C for 1 hr. They concluded that crystallization may proceed from either (1) the uniform distribution of elements in a dried gel which promotes the solid-state reaction by minimizing the diffusion distance for each element or (2) the accumulation of mechanical energy in the dried gel and the reaction promoted by the energy stored as dangling bonds in the gel network. Accumulation of mechanical energy in the gel structure seems to promote the formation of cordierite by increasing internal energy [17].

Kurama and Ay, proposed the use of two different sources of MgO and grinding times to form cordierite. In the first mix type, they used ultrafine precipitated $Mg(OH)_2$ with kaolin and in the second type of mix, they used talc with kaolin. These mixtures were prepared in a $MgO/Al_2O_3/SiO_2$ molar ratio of 1:1:2 and were ground using a planetary ball mill for 2 or 4 hrs. They, however, did not report the grinding speed. The samples were sintered at 1200^{o}C for 2 hrs. They concluded that the intensity of the cordierite peaks varied with grinding time. The amount of cordierite for both mix types increased with increased grinding time. The MgO source is also an important parameter for the formation of α-cordierite. Because the particle size of the precipitated $Mg(OH)_2$ was much smaller than that of the talc. This caused easier reaction of $Mg(OH)_2$ than talc with the kaolin [18].

In a more recent study, Tamborenea *et al.,* investigated the influence of mechanical treatment by grinding on the formation of cordierite from a talc, kaolinitic clay and gibbsite mixture. The mixture was ground by oscillating mill with a frequency of 12.5 s^{-1} for 5-20 min. According to this study, the crystalline structure of the raw material was lost and the reactivity increased owing to milling and finally cordierite was synthesized at 1215^{o}C [19].

Most recent work on the subject still lacked the high energy grinding necessary for mechanochemical synthesis [17-19].

3.1.2. MgO-Al_2O_3-SiO_2 System

A ternary system, which is important in understanding the behavior of cordierite ceramic composition is the MgO-Al_2O_3-SiO_2 system, is illustrated in Fig. 3.1. This system is composed of several binary compounds; Mullite ($3Al_2O_3.2SiO_2$), Enstatite ($MgO.SiO_2$), Forsterite ($2MgO.SiO_2$) and Spinel ($MgO.Al_2O_3$) together with two ternary compounds; Sapphirine ($4MgO.5Al_2O_3.2SiO_2$) and Cordierite.

Cordierite is situated in the primary crystallization field of mullite and has a chemical composition of MgO: 13.8, Al_2O_3: 34.8 and SiO_2: 51.4 (weight %). It has an incongruent melting point, because the solid compound of cordierite does not melt to form the liquid of its own composition, but instead dissociates to form the new solid phase and the liquid. The lowest liquidus temperature is at the tridymite-protoenstatite-cordierite eutectic at 1345^{o}C, but the cordierite-enstatite-forsterite eutectic at 1360^{o}C is almost as low-melting in the ternary system [21].

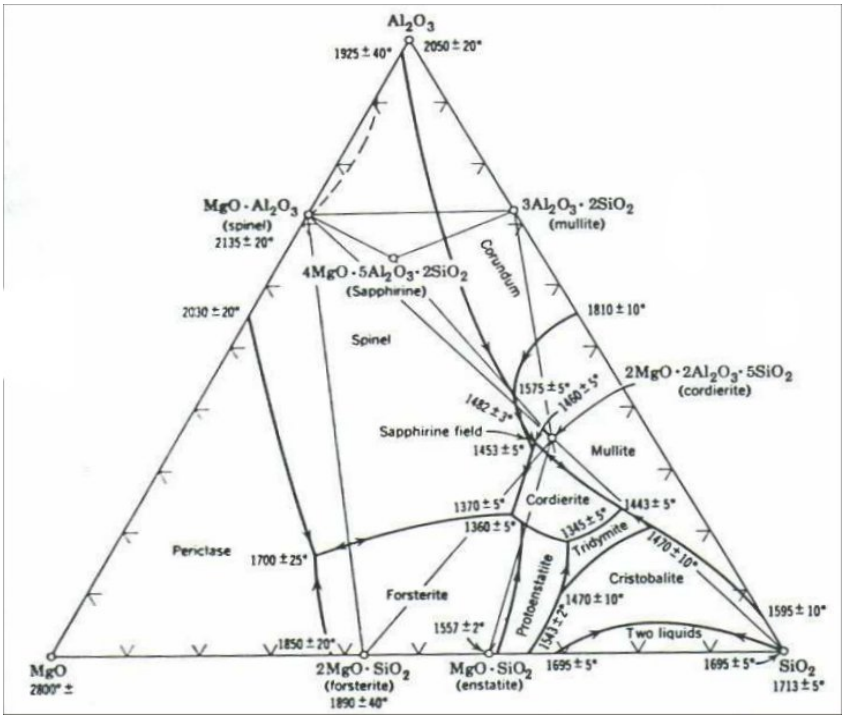

Figure 3.1. MgO-Al_2O_3-SiO_2 Ternary Phase Diagram [20].

3.1.3. Synthesis of Magnesium Borate

Most commercial ceramics are densified with a liquid phase present. A large number of ceramic components are used in low-temperature applications where the presence of a low-melting amorphous grain-boundary phase separating the crystalline grains is not critical. Examples include 96 % alumina substrates for computer packages, alumina or zirconia milling media, and alumina spark plug insulators. This amorphous phase arises from liquid formed during the sintering process whose function is to coat the powder particles and cause more rapid densification at temperatures much lower than are needed for solid state sintering [22].

Many electronic ceramics, which may be co-fired with metals at reduced temperatures, are formulated with low melting glasses as densification aids [3].

In the cordierite synthesis, some additives; B_2O_3 and P_2O_5 were used for increasing phase-transformation kinetics and increasing bulk density. Wu *et al.,* compared the effects of these on the cordierite synthesis. They prepared three batches. In the first one; 5 wt % B_2O_3, the second one; 2.5 wt % B_2O_3+ 2.5 wt % P_2O_5 and last one; 5 wt % P_2O_5 additives were used. They concluded that the addition of B_2O_3 enhances the α-cordierite formation much more than the addition of P_2O_5 [23].

Sumi *et al*., synthesized magnesium borate ($2MgO.B_2O_3$) by using boric acid (H_3BO_3) and $Mg(OH)_2$ solutions. Boric acid (H_3BO_3) solution and a synthesized $Mg(OH)_2$ solution were mixed in the molar ratio of $2MgO:B_2O_3$. After drying, the mixed powders were heated at a temperature of 700°C for 3 hrs and $2MgO.B_2O_3$ was obtained. Synthesized $2MgO.B_2O_3$ powders were bead-milled for 40 hrs using ethanol and zirconia (ZrO_2) beads that were 3 mm in diameter [14].

Kurama *et al.,* also used the same method. However, they mixed boric acid (H_3BO_3) solution with synthesized $Mg(OH)_2$ powders. After mixing, the same procedure was applied for $2MgO.B_2O_3$ synthesis [24].

3.2. Spinel

Spinel is the common name for the simple metal oxide structure that can be built up on the basis of nearly close-packed oxygen ions, with cations placed in available interstices. A number of oxides of general formula AB_2O_4 have cubic close-packed

structures. The oxygen ions are in face-centered cubic close packing arrangement. The structure of spinel is shown in Figure 3.2.

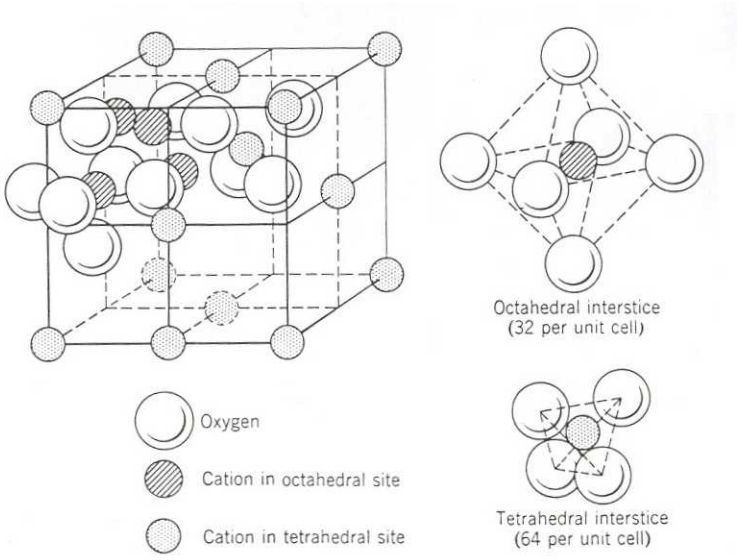

Figure 3.2. The structure of spinel [21].

Two types of spinel occur. In the *normal* spinel the A^{2+} ions are on tetrahedral sites and the B^{3+} ions are on octahedral sites. This structure was observed for $ZnFe_2O_4$, $CdFe_2O_4$, $MgAl_2O_4$, $FeAl_2O_4$, $CoAl_2O_4$, $NiAl_2O_4$, $MnAl_2O_4$ and $ZnAl_2O_4$. In the *inverse* spinels, the A^{2+} ions and half the B^{3+} ions are on the octahedral sites; the other half of the B^{3+} are on tetrahedral sites, $B(AB)O_4$. This is more common structure and is observed for $FeMgFeO_4$, $FeTiFeO_4$, Fe_3O_4, $ZnSnZnO_4$, $FeNiFeO_4$ and many other ferrites of importance for magnetic properties [21].

Magnesium aluminate spinel has a great importance as a structural ceramic owing to its use in refractories industry. It provides a combination of desirable physical, chemical and thermal properties, both at normal and elevated temperatures. Its published properties are given in Table 3.2. It melts congruently at 2135°C, shows high resistance to attack by most of the acids and alkalis and has low electrical losses. Due to these desirable properties, it has a wide range of application in structural, chemical, optical and electrical industries. It is used as a refractory lining in steel-making furnaces, transition and sintering zones of cement rotary kilns [25], checker work of the glass furnace regenerators [26] sidewalls and bottom of the steel ladles, glass furnaces and melting tanks.

Table 3.2. Main physical properties of spinel.

$T_{melting}$ (^oC)	**Density** (g/cm^3)	**Crystal structure**	**Lattice constant** (Å)	**Refractive index**	**Molecular Weight** (mg)
2135	3.64	Face-centered cubic	a = 8.08	1.71	142.27

Synthesis and fabrication of spinel $MgO.Al_2O_3$ has been known for a long time. A number of techniques such as conventional solid-state-reaction (SSR) [27], co-pecipitation [28] and gelation-precipitation process [29] have been extensively employed. Ping *et al.,* [30] stated in recent reports "The conventional SSR method is the most utilized one in spinel preparation. However, it has several disadvantages such as longer processing time, need for repetition of calcination stages, requirement of very high temperatures for sintering attended by non-uniform and abnormal grain growth and remnant porosity."

3.2.1. MgO-Al_2O_3 System

MgO-Al_2O_3 is a binary eutectic system as illustrated in Figure 3.3. It consists of two eutectics and an intermediate compound $MgAl_2O_4$. Some range of solid solution exists for periclase and spinel, while corundum dissolves negligible MgO. There is an extensive solid solution of Al_2O_3 in spinel that reaches a maximum of about 85 wt % Al_2O_3 at 1860^{o}C and a more limited solid solution of MgO in spinel reaching 62 wt % Al_2O_3 at 1995^{o}C. The solid solution field of the spinel phase is marked by "S" in Fig. 3.3. There also exists a substantial solid solution of Al_2O_3 in periclase endmember at elevated temperatures. On the other hand, at the corundum endmember no solid solution field is shown for MgO since the solubility of MgO in corundum is at most a few hundred parts-per-million [3].

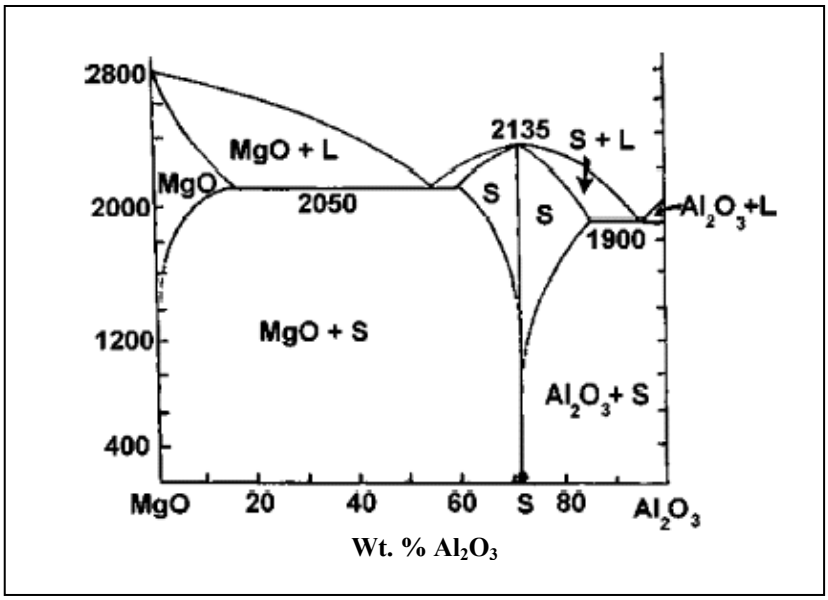

Figure 3.3. MgO-Al_2O_3 Binary Phase Diagram [31].

3.2.2. Spinel Synthesis

Tremendous amount of work was done on spinel synthesis. In this section, however, previous works on spinel synthesis that are most relevant to mechanochemical techniques are mentioned.

Mazzoni *et al.,* used relatively cheap raw materials of magnesium hydroxide ($Mg(OH)_2$) and gibbsite ($Al(OH)_3$) in their study. The raw materials were mixed to form a stoichiometric spinel composition, and then the mixture was mechanically activated by oscillating mill with frequency of 12.5 s^{-1} for different grinding durations from 5 to 15 min. In addition to the oscillating mill, they also used ball mill and vibratory mill to investigate the mechanical activation on spinel synthesis. The ground mixtures were heat treated between 650 to 1300^oC. They observed that mechanical effects lead to a progressive structural modification producing a disordered structure with high surface energy by defects and imperfections. According to their study, all mill types resulted in mechanochemical effects, which were shown by crystallinity loss, and structural modification of the components. These mills produced defects and imperfections favoring spinel formation. Spinel powders were synthesized at relatively low temperatures (850^oC) [32].

In the literature, Kostic *et al.,* presented the use of α-alumina and basic heavy magnesium carbonate ($(MgCO_3)_4.Mg(OH)_2.5H_2O$) for spinel synthesis. They mixed the

raw materials, ground by vibrating mill at 1000 rpm for 5-120 min. and heated at 800-1250^{o}C for 1 and 4 hrs in the form of pressed pellets (20 MPa). The study resulted in a decrease in spinel phase formation temperature by prolonged grinding. Mechanical activation was most pronounced in mixtures ground up to 30 min. and heated up to 900^{o}C. However, further mechanical activation grinding from 30 to 120 min. did not show any significant contribution at that temperature [33].

In another study, Kim and Saito, investigated the synthesis of spinel from a powder mixture of magnesium hydroxide ($Mg(OH)_2$) and gibbsite ($Al(OH)_3$) by changing grinding time and calcination temperatures. In this study, dry grinding using a planetary ball mill activated the raw materials. The mixture (4.0 g) was put in the mill pot and ground at 790 rpm in rotational speed of the mill. The duration of grinding was varied from 5 to 240 min. The ground mixtures were calcined at 600-1200^{o}C for 1hr. According to their study, crystallization of $MgAl_2O_4$ from the ground mixtures was detected at 780^{o}C when the mixtures were ground over 15 min [34].

In a more recent study, Plesingerova *et al.,* considered the effect of mechanical activation of various reacting raw materials. The degree of conversion to $MgAl_2O_4$ spinel of homogenized mixtures of Mg and Al oxides and/or hydroxides was compared with the mechanically activated mixtures of these initial powders after firing in the temperature range of 600-1200^{o}C. Mechanical activation was carried out in high-speed planetary ball mill (acceleration 5.44 g) for 10 hrs in air. As a result of their study, mechanochemical activation decreased the temperature of conversion to $MgAl_2O_4$ spinel via comminution, reduction of primary particles, formation of soft, dense agglomerates, enlargement of grain boundary areas, and possible amorphization and mechanochemical dehydration. Due to these reasons, binary mixture of $Mg(OH)_2$ and $Al(OH)_3$ showed the best interaction between components of the mixture. This significantly stimulates solid-state reactions to $MgAl_2O_4$ spinel during subsequent heating, even at a temperature of 800^{o}C [35].

CHAPTER 4

EXPERIMENTAL

In this chapter, the materials and methods used in cordierite and spinel synthesis and their characterization techniques are presented.

4.1. Materials

Different sources of raw materials were used for cordierite and spinel synthesis. These raw materials are explained in more detail in the following sections. Their physical and chemical properties are listed in Tables 4.1 and 4.2.

Reagent grade aluminium hydroxide ($Al(OH)_3$) (MERCK) and magnesium hydroxide ($Mg(OH)_2$) (SIGMA) were used as raw materials for spinel synthesis.

Sivas Kaolin, Egyptian Talc, reagent grade aluminium hydroxide (Gibbsite) ($Al(OH)_3$) (MERCK) and alumina (Al_2O_3) (AlCOA CT3000SG) were used as raw materials for cordierite synthesis.

Sivas Kaolin ($Al_2O_3.2SiO_2.2H_2O$)**:** Kaolin is the most common mineral in the production of cordierite [14-16, 18, 19]. It is used as a source of SiO_2 and Al_2O_3. Kaolin increases the plastic behaviour of the batch. Sivas kaolin was recently studied for its composition and mineralogical characteristics [36]. It was chosen as a component in this study because of its low impurity content. It was found to contain some quartz based on its X-ray diffraction analysis. The XRD data are not shown here for the sake of brevity.

Egyptian Talc ($3MgO.4SiO_2.H_2O$)**:** Talc was used as the source of MgO and SiO_2 in the production of cordierite. Talc has also been used as the main raw material for cordierite synthesis in many studies [15, 16, 18, 19].

Superground Alumina (Al_2O_3) (AlCOA CT3000SG)**:** It is widely employed in electronics industry as a dielectric substrate material, was used as the source of alumina in this study [15, 23]. The addition of alumina to cordierite batch increases the refractoriness of the mixture.

Aluminium Hydroxide: Another material that was used as a source of Al_2O_3 in cordierite [16, 19] and spinel [27, 28, 34, 35] synthesis was reagent grade aluminium hydroxide (Gibbsite) ($Al(OH)_3$) (MERCK).

Magnesium Hydroxide: Reagent grade magnesium hydroxide ($Mg(OH)_2$) (SIGMA) was used as the source of MgO in spinel synthesis [27, 34, 35].

Synthesized Magnesium Borate ($2MgO.B_2O_3$)**:** Magnesium borate was used as an additive to decrease cordierite synthesis temperature. In this study, magnesium borate powder was produced in-house by mixing boric acid (H_3BO_3) solution and magnesium hydroxide $Mg(OH)_2$ powder. Boric acid solution and reagent grade magnesium hydroxide powder were mixed in molar ratio of $2MgO:B_2O_3$. Reagent grade boric acid (SIGMA) powder and reagent grade magnesium hydroxide (SIGMA) powder were used as raw materials. 5 g of boric acid powder was dissolved in 400 ml deionized water. After complete dissolution, 4.72 g of magnesium hydroxide powder was added to the solution. To evaporate the water, the solution was stirred on the hot plate. To completely evaporate water, the solution was kept in the oven at 80^oC for 24 hrs. The loose powder mixture was heated at 700^oC for 3 hrs. The synthesized mixture was examined by X-ray diffraction method to confirm total conversion into magnesium borate. The synthesized magnesium borate was ground in planetary mono mill for 30 min. at 300 rpm to decrease the particle size. Ground powder was also examined by x-ray diffraction and particle size examination was done on electron microscope (SEM) images. These results are not shown here for the sake of brevity.

4.2. Method

4.2.1. Powder Mixture Preparation

In this part, the methods employed for synthesis of powders are explained.

Powder mixture preparation for spinel synthesis: Aluminium hydroxide and magnesium hydroxide were mixed in stoichiometric proportions to attain spinel composition. 7 g of mixture was weighed. According to calculation 5.2 g of aluminium hydroxide was mixed with 1.8 g of magnesium hydroxide.

Powder mixture preparation for cordierite synthesis: Before investigating the grinding affects on the cordierite synthesis temperature we first examined the source of alumina (Al_2O_3 or $Al(OH)_3$) and mixture mole ratio (1:1:2 or 2:2:5) $MgO\text{-}Al_2O_3\text{-}$

SiO_2 for cordierite. In the literature, some researchers have employed a 1:1:2 mole ratio [15, 16] while some others have used a 2:2:5 mole ratio [14, 18]. Many different raw materials were used for cordierite synthesis in previous studies. The kaolin and talc were most common minerals in the production of cordierite, as a source of silica (SiO_2) and magnesia (MgO), respectively. However, to determine the alumina source, two different sources, alumina and aluminum hydroxide were investigated. In addition to determining the source of alumina, the mixture mole ratio was also investigated. Therefore two different mole ratios were employed in this project.

The mixtures, which were prepared with different sources of alumina and mole ratios, are listed in Table 4.3.

Table 4.1. Chemical analyses of used raw materials [36-38].

	Egyptian Talc Published Analysis (OMYA)	**Sivas Kaolin**	**CT3000SG Alumina (ALCOA)**
Al_2O_3	0.94	33.07	99.6
SiO_2	58.94	52.86	0.03
MgO	31.18	0.00	0.09
Na_2O	0.00	0.13	0.08
K_2O	0.00	0.12	0.00
CaO	1.57	0.47	0.02
Fe_2O_3	0.40	0.05	0.02
TiO_2	0.00	0.38	0.00
MnO	0.00	0.10	0.00
SO_3	0.00	0.60	0.00
B_2O_3	0.00	0.00	0.00
LOI	6.97	12.22	0.16
Total	100.00	100.00	100.00

Table 4.2. Physical properties of as-received raw materials [36-38].

	E. Talc (OMYA)	**Sivas Kaolin**	**Alumina (AlCOA)**	**Aluminium hydroxide ($Al(OH)_3$)**	**Magnesium hydroxide ($Mg(OH)_2$**
Density (g/cm^3)	2.7	2.62	3.9	2.42	2.36
Molecular Weight	434.3	258.16	102	77.99	58.32
Particle size (μm)	d_{50}=13	<106	d_{mean}=0.85	-	-

Table 4.3. The mixtures design chart for cordierite synthesis.

		Source of alumina	
		Al_2O_3	$Al(OH)_3$
mole ratio MgO: Al_2O_3: SiO_2	1:1:2	**M1**	**M3**
	2:2:5	**M2**	**M4**

These mixtures (15 g) were wet ground in 50 ml deionised water in the planetary mono mill for 30 minutes at 300 rpm to obtain homogenised mixtures. The slurry was spread on tray and dried in the oven at 80°C for 24 hrs. These mixtures were fired at different temperatures from 1200 to 1300°C for 1hr.

4.2.2. Grinding

Mechanochemical activation was applied with planetary mono mill (Fritsch Pulverisette 6). A photograph of the device is shown in Figure 4.1.

Grinding for spinel synthesis: Spinel mixture was ground as follows; six sintered corundum (Ø: 20 mm) balls were used as the grinding media in a 250 ml sintered corundum mill container. The mixtures were ground at 600 rpm for varying durations from 5 to 230 minutes. The equipment was paused after every 15 minutes of operation in order to avoid excessive heating. In the second set of experiments, 10 g of sample was ground for 60 minutes at 600 rpm in the same grinding conditions.

Grinding for cordierite synthesis: Full factorial experimental design was applied for cordierite synthesis. Cordierite mixture was ground as follows. Thirty tungsten carbide balls (Ø: 10 mm) were used as the grinding media in a 250 ml tungsten carbide mill container. Grinding time (minute) and grinding rotational speed (rate per mimute) were design parameters. These were changed from 300-500 rpm and 15-60 minutes, grinding rotational speed and time, respectively.

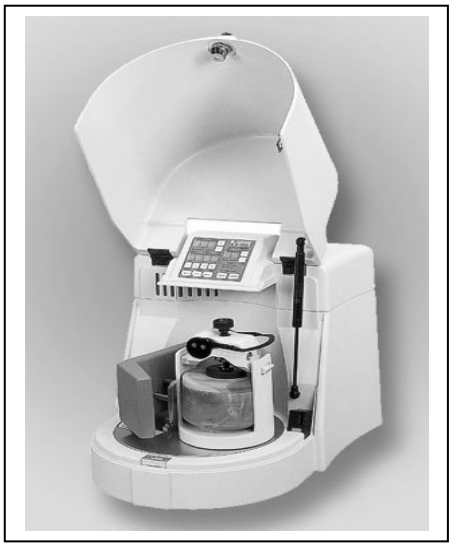

Figure 4.1. Planetary mono mill.

4.2.3. Compaction

Mechanically activated powder mixture for cordierite synthesis was uniaxially pressed (Yıldız Hidrolik San. Tic, 2001 Model) at 120 MPa in a stainless steel die (D:12 mm).

4.2.4. Heat Treatment

The loose powders for spinel synthesis and compacted pellets for cordierite synthesis were heated in a 5 liter globar benchtop kiln (Alser Teknik A.Ş. Protherm PLF 160/5). A photograph of the kiln is shown in Figure 4.2. An "S" type thermocouple was used for temperature measurement.

Figure 4.2. Globar benchtop kiln.

Heat treatment for spinel synthesis: 10 g specimens for spinel synthesis were first ground at 600 rpm for 60 minutes, and was subdivided into 1g samples which were later heat treated in an alumina crucible in loose powder form at varying temperatures (600-1400^{o}C). The soak time was 2 hrs, and the heating rate was 5^{o}C/min. The kiln was allowed to cool by itself.

Heat treatment for cordierite synthesis: The pelletized cordierite mixtures were heated in a temperature range of 1000-1300^{o}C. The soak time was varied from 1-4 hrs. The heating rate was 10^{o}C /min. The kiln was allowed to cool by itself.

4.3. Statistical Experimental Design

Laboratory cordierite synthesis tests were planned by the use of statistical experimental design. The objective was to determine the effect of factors influencing the synthesis process. The key in statistical experiment design is that it enables the researcher to obtain maximum possible amount of information from a limited number of runs. Because of the cost of experimentation in high temperature heating, the statistical design is valuable.

In this thesis we started with the initial series of 8 experiments designed according to the 2^3 full-factorial experiment design using the factors listed in Table 4.4. The aim was to identify the more important factor effects in addition to recognizing if there is any significant interaction between the factors. This kind of experiment design

is used by several researchers, and it uses the complete 2^p factorial experiments where p is the number of factors [39]. The 2 means that each factor is tested at two different levels. The results can provide the significant main effects, two factor interactions and also three factor interactions clear of each other. The experiments were done under the conditions that are listed in Tables 4.4. and 4.5 and Figure 4.3. The factors were coded as A: grinding speed (rpm), B: grinding time (minutes) and C: heating temperature (^oC).

Table 4.4. Screening experiment design planned.

Factor	Low level	High level
A: Grinding speed (rpm)	300	500
B: Grinding time (min)	15	60
C: Heating temperature (^oC)	1100	1200

Table 4.5. Experimental conditions in 2^3 full factorial design.

Run#	A: Grinding speed (rpm)	B: Grinding time (min)	C: Heating temperature (^oC)
1	300	15	1100
2	500	15	1100
3	300	60	1100
4	500	60	1100
5	300	15	1200
6	500	15	1200
7	300	60	1200
8	500	60	1200

The potential response variables were cordierite peak height and peak area in the x-ray diffraction chart, and exothermic peak area in the DTA plot. In this project, the peak intensity for cordierite in the XRD chart was used as response variable.

Other additional sets of experiments were done for the purpose of comparing the effect of heating temperature and additives on the formation of cordierite.

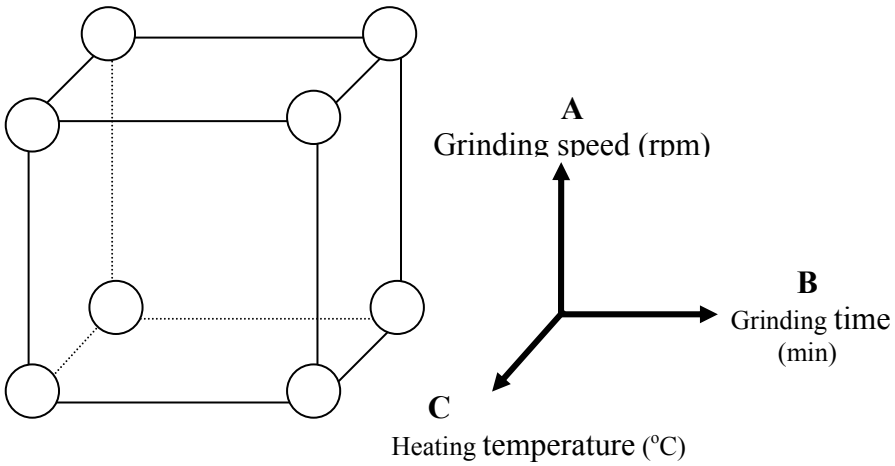

Figure 4.3. Design cube used in 2^3 full factorial experiments.

4.4. Product Analysis

4.4.1. X-Ray Diffraction Analyses

X-ray diffraction (XRD) with Cu Kα radiation (λ=1.54 A) was used to detect the present phases and crystallinity of the ground and heated mixtures (Philips X'pert Pro, XRD).

X-ray intensity was determined by the diffraction peak heights using the positions listed in Table 4.6.

Table 4.6. JCPDS card numbers and peak positions used for XRD peak intensity measurements.

Mineral	JCPDS number	(hkl)	Diffraction angle (2θ)
α-Cordierite	82-1884	(100)	10.44^o
Spinel	03-0901	(440)	65.18^o

4.4.2. Differential Thermal Analyses (DTA)

DTA analysis was carried out in order to investigate thermal behaviour of the mixtures (Shimadzu DTA-50, Japan). Heating was done under argon gas atmosphere at a rate of 10^oC/min.

4.4.3. Microstructural Analyses (SEM)

The morphology and particle size of the mixtures were observed by scanning electron microscope (Philips XL-30S FEG, SEM).

4.4.4. Fourier Transform Infrared (FTIR) Spectroscopy

FTIR spectra were obtained using a Shimadzu FTIR 8601 PC spectrometer. The sample was prepared by thoroughly mixing 4 mg of powder with 200 mg of KBr (IR Grade). FTIR studies were performed in the wavenumber range 4600-400 cm^{-1}. Spectra were obtained by co-addition of 40 individual scans.

4.4.5. Density and Porosity Measurements

The density and porosity of the synthesis cordierite mixtures were determined using Archimedes' technique (ASTM C 20-87) [40]. This method covers the determination of the following properties of products: apparent porosity, water absorption, and bulk density. The density and porosity were measured on the balance with Archimedes' apparatus (Precisa-XP220A).

CHAPTER 5

RESULTS AND DISCUSSION

In this chapter, the results obtained from spinel and cordierite synthesis experiments are presented and discussed. In the first part of this chapter, the results of spinel synthesis experiments are presented. Spinel phase formation was analyzed via X-ray diffraction analysis and grinding affects on the raw materials' crystalinity was examined with DTA (Differential Thermal Analysis). Particle size and morphology of ground powders were investigated by SEM.

In the second part, results of cordierite synthesis experiments are reported. Due to the large number of parameters that may affect the synthesis of cordierite, SED (Statistical Experimental Design) techniques were implemented. The powder amorphization and cordierite synthesis were tracked by x-ray diffraction and DTA methods. The bonding structure of ground mixture and synthesized cordierite were investigated by FTIR. The particle size and morphology of powders and synthesized cordierite crystals were observed by SEM.

5.1. Spinel Synthesis

As explained in Chapter 4, mixtures of analytical grade $Mg(OH)_2$ and $Al(OH)_3$ were prepared in stoichiometric proportions and were ground for prescribed periods of time at different speeds in a planetary mono mill.

5.1.1. X-Ray Diffraction Analyses

XRD patterns of mixtures, which were ground at different grinding times, are shown in Figure 5.1. Note that all XRD patterns reported in this thesis were generated from CuKα radiation that has a wavelength of 0.1542 nm. Intensities of raw materials decrease with increased grinding time and amorphization of the starting materials is completed within about 50 minutes. After 110 min of grinding, new phases of spinel and corundum were observed in the XRD pattern [41]. Stronger peaks for corundum were observed with increasing grinding times because of wearing of sintered corundum

pot and the grinding media. 230 minutes of grinding resulted in severe contamination of mixture by corundum from the pot and stronger corundum peaks overshadowed the spinel phase.

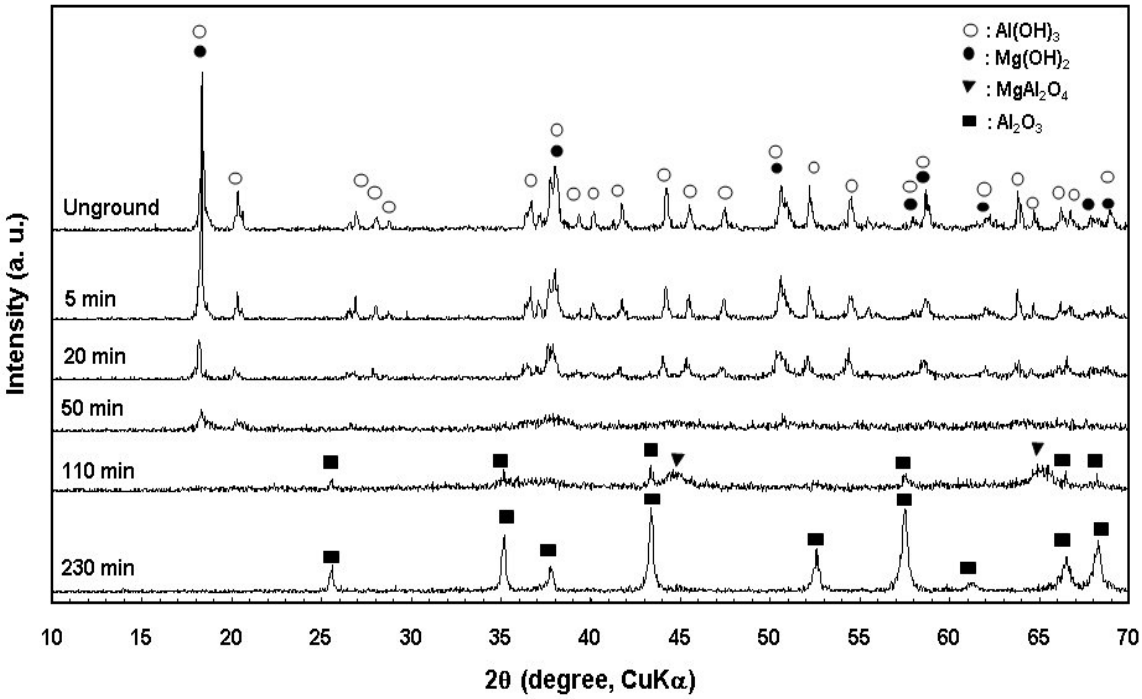

Figure 5.1. XRD pattern of the mixtures ground for various durations.

Figure 5.2 shows the XRD patterns of the 60 min ground mixtures, which were heat treated at different temperatures. The peaks of the raw materials did not disappear completely after 60 min of grinding since the amount of starting raw materials of 60 min ground sample (10 g) was much higher than that of the previously 50 min ground sample (4 g) which could reach complete amorphization. The latter is shown in Figure 5.1.

However, when the mixture was heated at 600°C, the original peaks of $Mg(OH)_2$ and $Al(OH)_3$ disappeared. When the calcination temperature went up to 800°C, several bumps in the XRD patterns were observed. These bumps were attributed to the periclase and spinel phases (Figure 5.2). Further heating led to the disappearance of the periclase phase upon reaction with alumina, and the subsequent formation of spinel at T>1000°C. At 1200°C and 1400°C, spinel peak intensities became even higher than that of 1000°C heated sample.

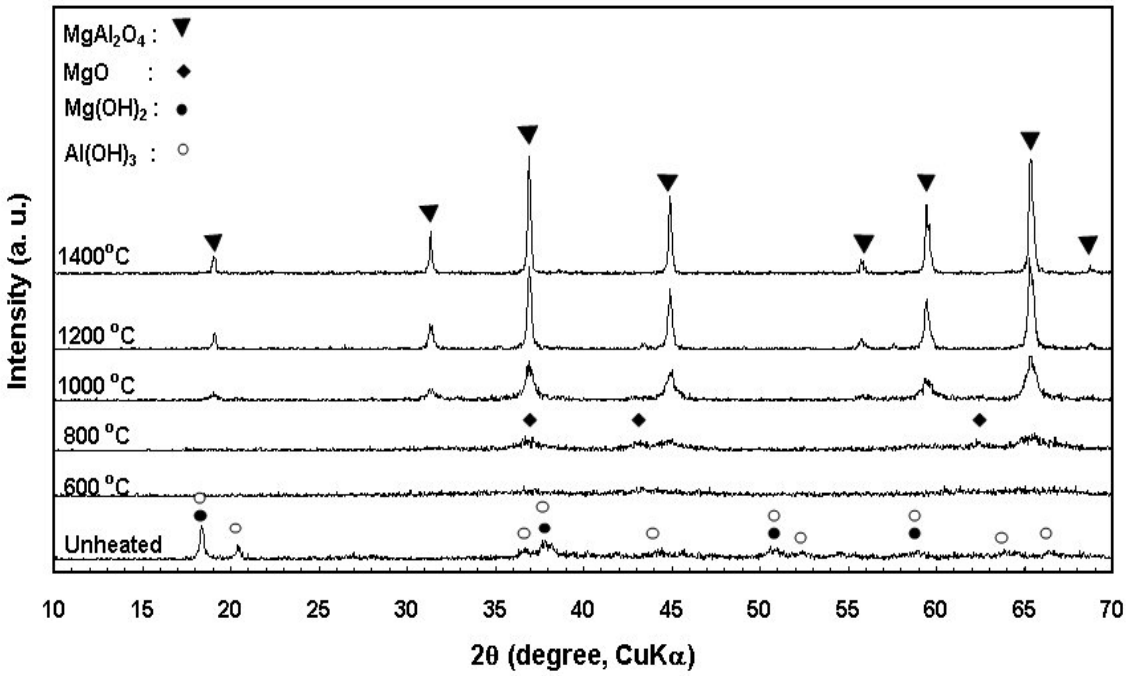

Figure 5.2. XRD patterns of the 60 min ground mixtures calcined at different temperatures.

5.1.2. Differential Thermal Analyses (DTA)

DTA analyses were also performed on the same samples. Results shown in Figure 5.3 supported the findings of XRD analyses. Loss of structurally bound water from Al and Mg hydroxides was detected at 310 and 390°C, respectively. A peak at nearly 255°C that was observed in the intermediate step of the gibbsite dehydration is noticeable in the unground and 5 min. ground samples but not in further ground samples. These peak positions slightly shifted to lower temperatures on increasing grinding times. The endothermic peak intensities also decreased on further grinding. After 230 minutes, there was no peak on the DTA chart, suggesting a completely dehydrated powder mixture.

5.1.3. Microstructural Analyses (SEM)

Secondary electron images of selected powder samples are shown in Figure 5.4. Significant particle size reduction was achieved after 5 min of grinding (Figure 5.4-b). Further reduction occurred at 50 and 110 min of grindings. Due to the fine particle size the powders tended to form agglomerates

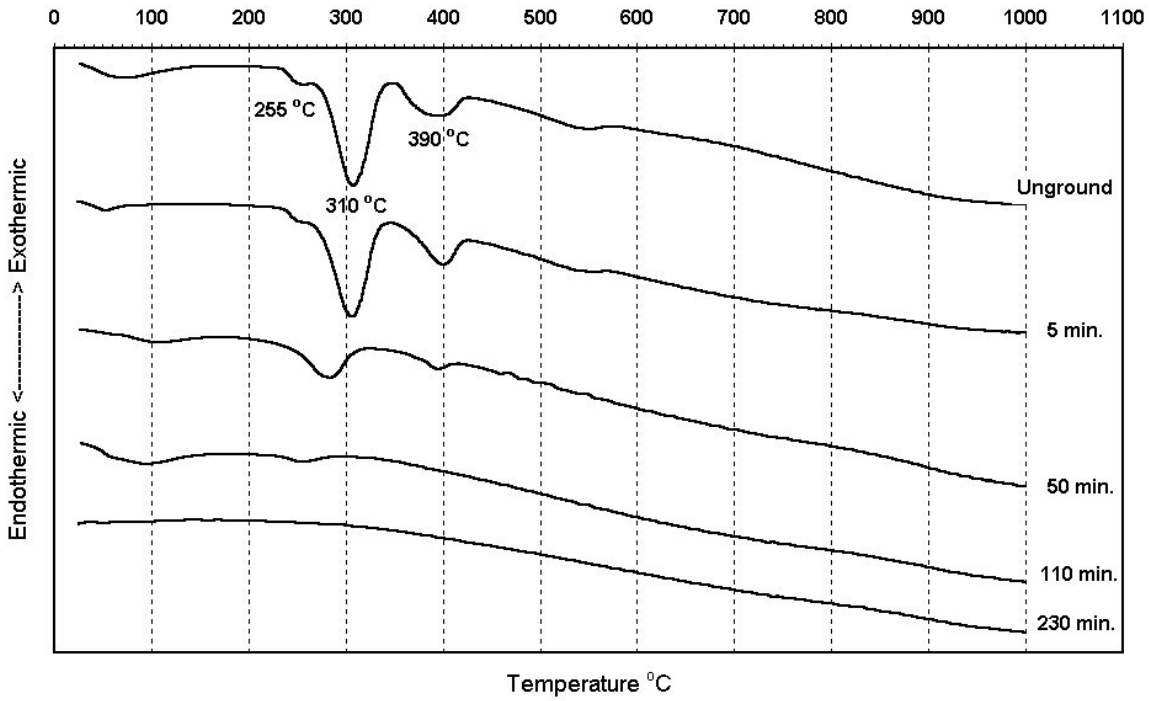

Figure 5.3. DTA analysis of ground mixtures.

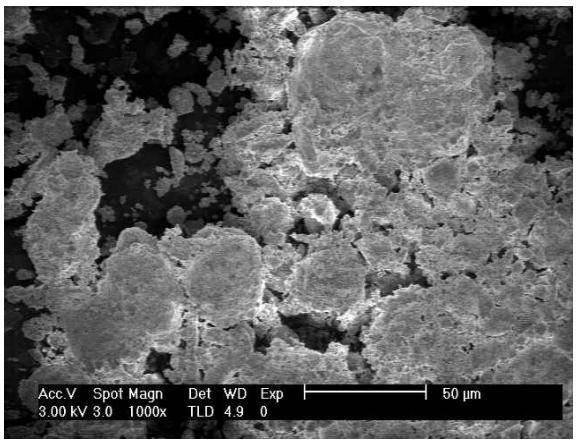

(a) Unground powder mixture

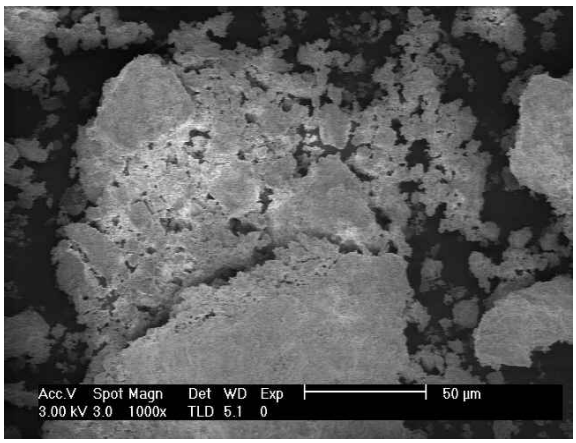

(b) After 5 minutes of grinding

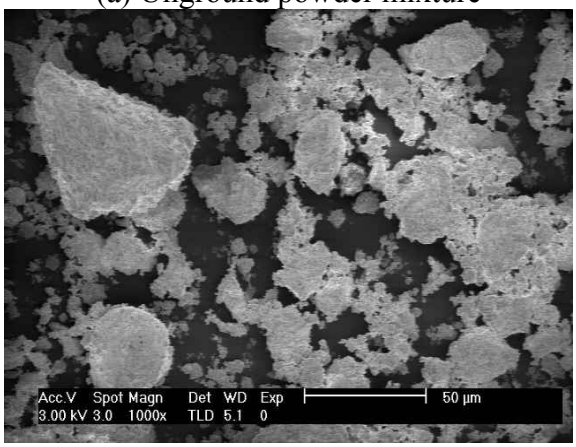

(c) After 50 minutes of grinding

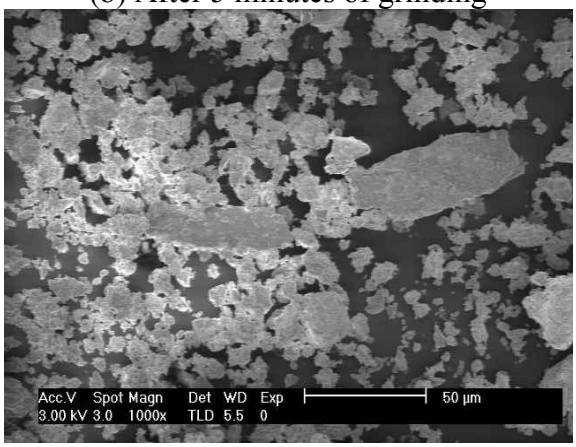

(d) After 110 minutes of grinding

Figure 5.4. SEM micrographs of powder specimens ground at 600 rpm

5.2. Cordierite Synthesis

Powder mixtures coded M1, M2, M3 and M4 were prepared to determine the suitable type of mixture molar ratio and alumina source for cordierite synthesis. Some of these mixtures were heated without being ground, while the majority of the samples were ground in a planetary mill before being compacted and heated in the kiln at high temperature. Soak temperatures varied from 1000 to 1300^{o}C and soak times were from 1-4 hrs. An additive was used in some samples to investigate its effect on cordierite phase formation.

5.2.1. Coding System Used for Samples in Cordierite Synthesis

Because of the large number of samples studied in the following sections, a coding system was used. There were a total of six parameters that were studied:

1) Powder mixture type (M1-M4),
2) Grinding rotational speed (0-500 rpm),
3) Grinding duration (0-60 minutes),
4) Soak temperature (0-1300^{o}C),
5) Soak time (0-4 hrs),
6) Percentage additives used (0-5 wt% $2MgO.B_2O_3$).

For example, the sample coded as M3-300-60-1150-4-0 indicates that an M3 mixture was prepared and ground at 300 rpm for 60 minutes in the mill before compaction in a cylindrical die. The pellet was then heated in a kiln at 1150^{o}C for 4 hrs. No additive was used for this sample.

5.2.2. X-Ray Diffraction Analyses

The XRD analyses results are shown in Figures 5.5 and 5.6, respectively. According to the x-ray results in Figure 5.5, cordierite was not detected in samples heated at 1200^{o}C for 1hr. In this temperature, raw materials did not completely react with each other to produce the desired phase. On the other hand, spinel, magnesium silicate, corundum and cristobalite were detected in the x-ray diffraction patterns. Corundum could not react with kaolin and talc at 1200^{o}C in 1hr. Silica transformed into

the cristobalite phase. So cordierite was not synthesized by classical solid state synthesis at this temperature.

X-ray diffraction patterns of the specimens fired at 1300°C for 1hr are shown in Figure 5.6. Cordierite and a small amount of spinel were detected in all of the specimens. In M2-0-0-1300-1-0 specimen, some cordierite main peaks existed but the major peak (Intensity 100) at 10.44° was not as strong. This is thought to originate from the preferential alignment of powder during XRD sample preparation.

According to these results, 1:1:2 mole ratio and $Al(OH)_3$ source provide better results than 2:2:5 mole ratio and Al_2O_3 source for cordierite synthesis. In addition to these results, adding Al_2O_3 is successful only if high temperature and long soak times are used; at lower soak times and temperature, the Al_2O_3 only partially reacts and corundum which is a high expansion, brittle phase, remains as an undesirable product [42].

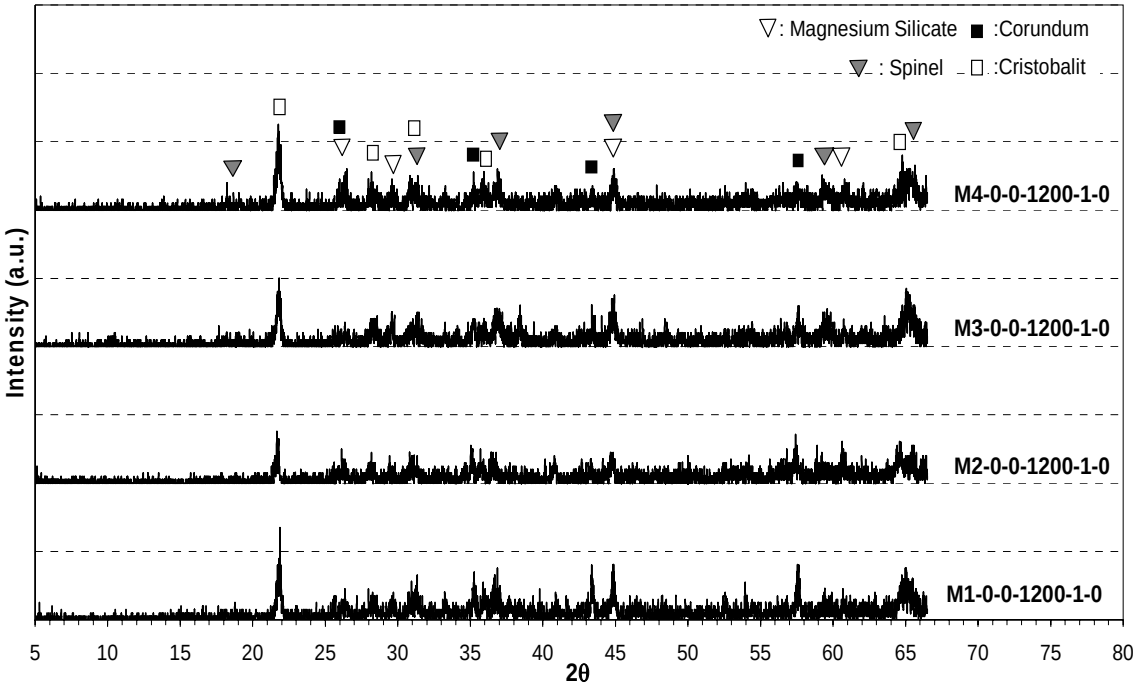

Figure 5.5. XRD patterns of the mixtures heated at 1200°C for 1hr.

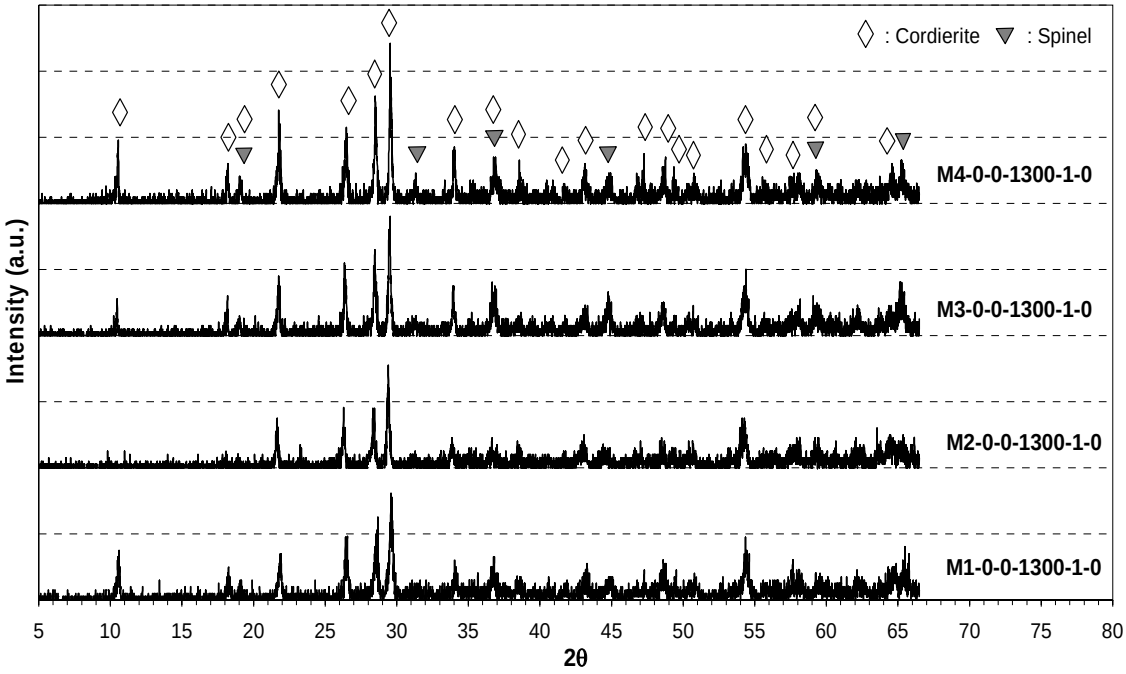

Figure 5.6. XRD patterns of the mixtures heated at 1300^{o}C for 1hr.

5.2.2.1. Experimental Design for Mechanochemical Synthesis of Cordierite

Based on the experiments with different precursors and mole ratios for cordierite synthesis, we selected the M3 mixture to investigate the effect of grinding for 1:1:2 mole ratio mixtures and $Al(OH)_3$ as a source of alumina (see Table 4.3). In order to minimize the number of runs experimental design methodology was employed. The grinding time, rotational speed and heat treatment temperature were selected as the design parameters. The soak time was 4 hrs, heating rate was 10^{o}C/min, grinding feed to media volume ratio (1:3) and ball size (ϕ:10 mm) were all fixed.

The single replicate of the 2^3 design was generated using commercial software called Design-Expert 6.0. A full factorial experiment was carried out for cordierite synthesis to study the factors thought to have influence on the synthesis rate. The three factors are grinding speed (A), grinding duration (B), and soak temperature (C). Each factor was studied at two levels. The design matrix is shown in Table 5.1.

Table 5.1. Experimental Design.

			High 1200°C	Low 1100°C
Rotational speed Low 300 rpm	High 60 min. grinding	M3-300-60-0-0-0	M3-300-60-1200-4-0	M3-300-60-1100-4-0
	Low 15 min. grinding	M3-300-15-0-0-0	M3-300-15-1200-4-0	M3-300-15-1100-4-0
Rotational speed High 500 rpm	High 60 min. grinding	M3-500-60-0-0-0	M3-500-60-1200-4-0	M3-500-60-1100-4-0
	Low 15 min. grinding	M3-500-15-0-0-0	M3-500-15-1200-4-0	M3-500-15-1100-4-0

XRD patterns for as-mixed M3 and ground mixtures (M3-300-15-0-0-0 to M3-500-60-0-0-0) are shown in Figure 5.7. Other samples that were heat treated were coded M3-300-15-1200-4-0 to M3-500-15-1100-4-0.

As was expected for the M3 mixture, raw materials kaolinite, talc and gibbsite were detected. As shown in Figure 5.7 for sample M3-300-15-0-0-0, the peak intensities of raw materials decreased. Further grinding of this mixture resulted in a completely amorphized powder. The crystal structures of talc, kaolinite and gibbsite were destructed. Samples that were ground more vigorously then 300 rpm and 60 min were all totally amorphized (See Fig. 5.7).

These ground mixtures (M3-300-15-0-0-0 to M3-500-60-0-0-0) were later fired at 1100°C and 1200°C for 4 hrs, and the resulting XRD charts are shown in Figures 5.8 and 5.9, respectively.

Small amount of cordierite phase was detected in the M3-300-60-1100-4-0 and M3-500-15-4-0 specimens in addition to main spinel and cristobalite phases in Figure 5.8. Hence, the 1100°C heat treatment was not sufficient for cordierite synthesis. At that temperature, the raw materials did not completely react with each other.

On the contrary, all samples that were heated at 1200°C (M3-300-15-1200-4-0 to M3-500-60-1200-4-0) showed cordierite and a small of amount spinel phase.

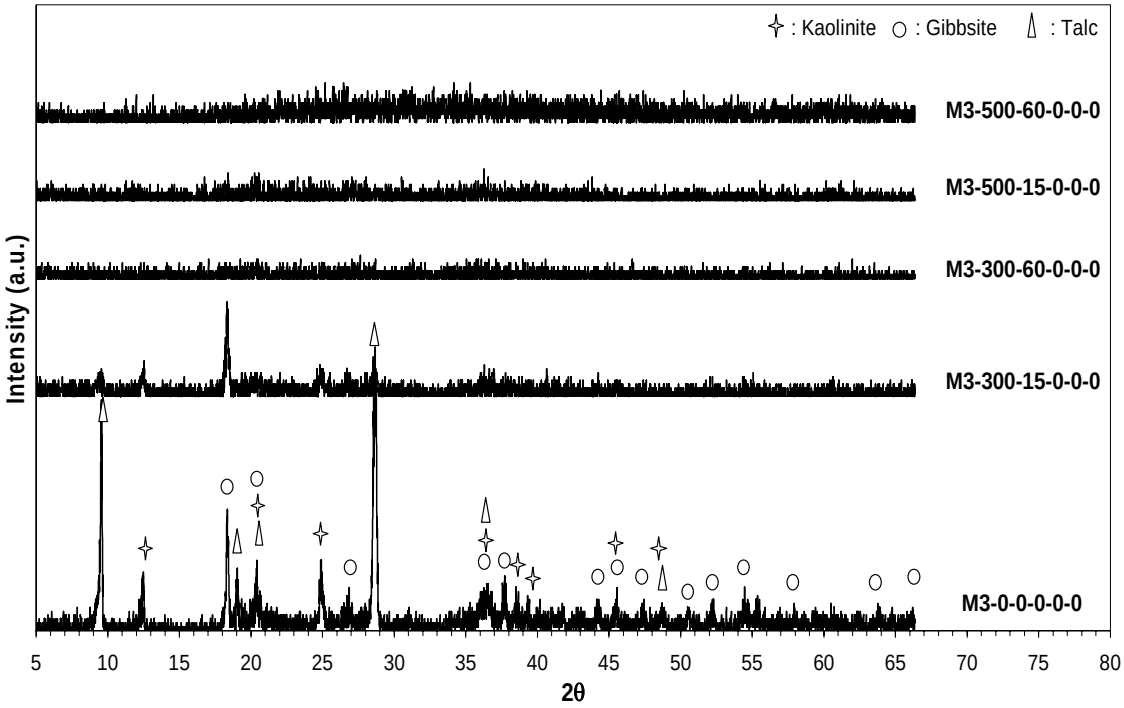

Figure 5.7. XRD patterns of the M3 samples that were ground at different conditions.

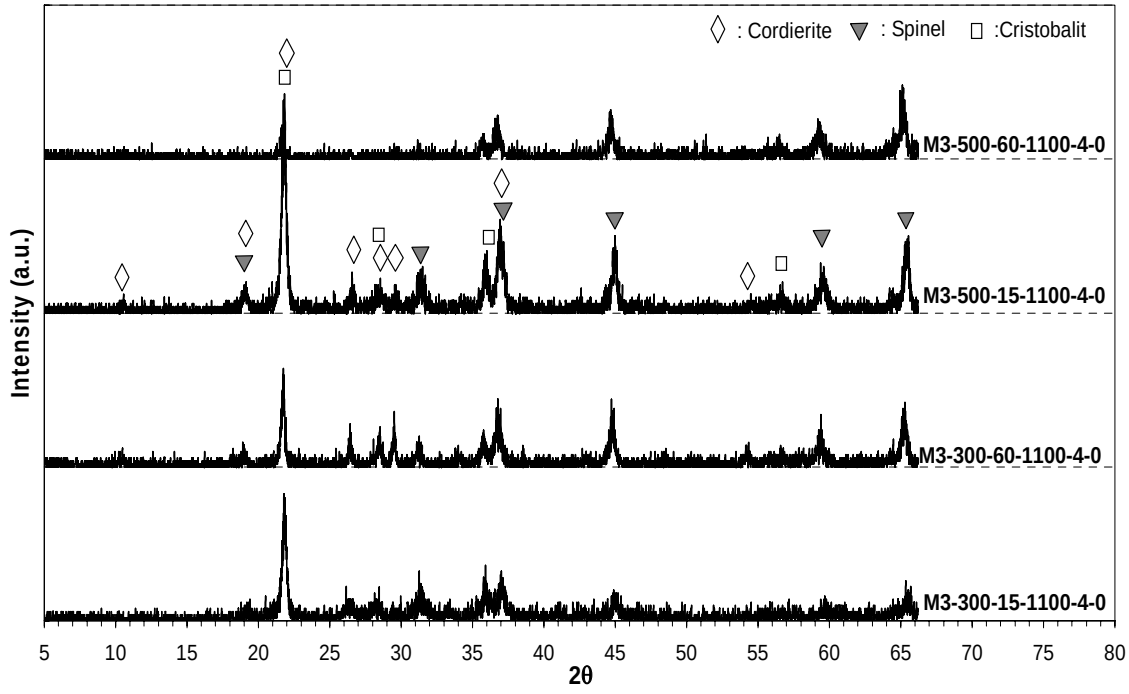

Figure 5.8. XRD patterns of the ground M3 samples that were heat treated at 1100^{o}C.

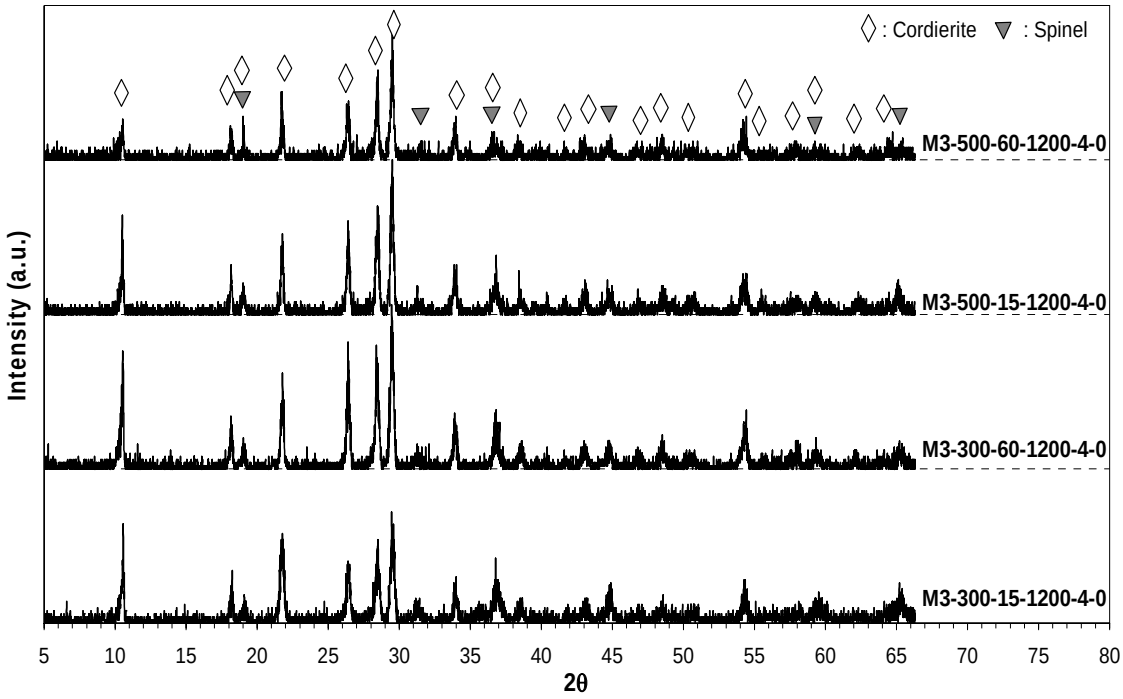

Figure 5.9. XRD patterns of the ground M3 samples that were heat treated at 1200^{o}C.

The data obtained from a single replicate of the 2^3 factorial experiment are shown in Table 5.2 and Figure 5.10. The values for the response variable were measured from the main peak intensities of cordierite in the XRD patterns in Figures 5.8 and 5.9. The 8 runs were made in random order. In Figure 5.10, the design cube that demonstrated the effects of factors on the response variable is shown.

Table 5.2. Results of designed set of experiments for cordierite synthesis.

Run Number	Factor			Run label	Response
	A	B	C		
1	-	-	-	(1)	0.00
2	+	-	-	A	6.15
3	-	+	-	B	4.03
4	+	+	-	ab	0.00
5	-	-	+	C	30.13
6	+	-	+	ac	44.96
7	-	+	+	bc	63.81
8	+	+	+	abc	16.99

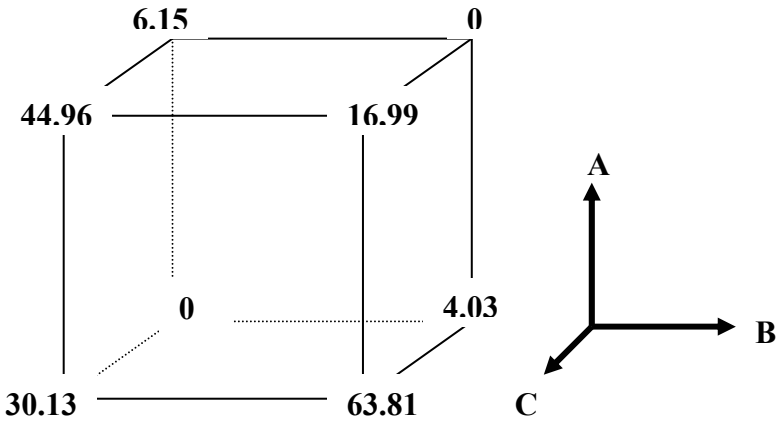

Figure 5.10. Values of the response variable peak intensity shown on the design cube.

The normal probability plot of these effects is shown in Figure 5.11. Such plots graphically show the significant factor effects that are positioned away from the diagonal line. If a factor effect is located near this line, then its effect on the response is statistically insignificant. The important effects that emerge from this analysis are the main effects of C (soak temperature), and then AB interaction (grinding speed and grinding time) and maybe ABC interaction.

The statistical analyses results (ANOVA table) for the cordierite synthesis rate data are given in Table 5.3. The sum of squares is used as a measure of overall variability in the data. The value of 3894.64 indicates that the variation in the experiment data is very large. Mean square values are obtained by dividing the sum of squares by the degrees of freedom. The model F-value of 402.92 implies that the model is significant. There is only a 3.81% chance that a "Model F-Value" this large occurs due to noise. The importance of each term, i.e., the influence of cross interaction between/among the components on the cordierite synthesis rate is shown by the values in column "Prob > F". Values of "Prob > F" less than 0.05 indicate that model terms are significant at the 95% confidence level. In other words we are 95% confident that the particular effect is significant. In this case, the main effect soak temperature (C) has the largest influence on the cordierite synthesis since the value of Prob > F is the smallest for model term C (p=0.0157). AB and ABC interactions are also significant at the 95% level.

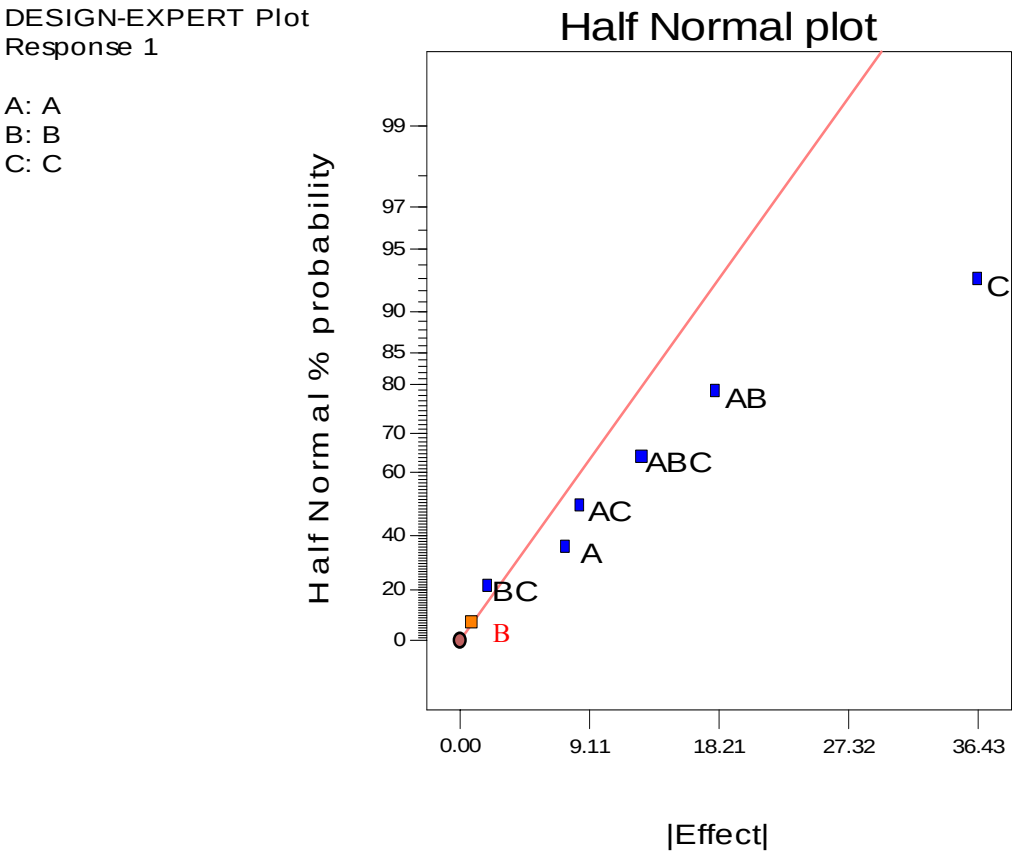

Figure 5.11. Normal probability plot of the effects for the 2^3 factorial.

According to the model, B (grinding duration) factor is not signifacant within the interval studied (15 and 60 min). As was indicated in Figure 5.7, there is no difference in the XRD patterns of M3-500-15-0-0-0 and M3-500-60-0-0-0 mixtures. A wider interval like 5-60 minutes may have created a significant factor effect.

AB interaction, however, is moderately significant. This means that the effect of grinding speed is different for different grinding durations.

After these experiments, we determined that the heat treatment temperature was the important parameter for cordierite synthesis. To investigate the heat treatment temperature in more detail, the specimens were heated at 1150°C for 4 hrs, and the results are shown in Figure 5.12.

Figure 5.12 clearly shows the effect of grinding and the contribution of mechanochemical action on the synthesis of cordierite. Samples M3-300-15-1150-4-0 to M3-500-60-1150-4-0 were all able to produce cordierite at 1150°C. However, the as mixed M3-0-0-1150-4-0 mixture was unable to produce cordierite after heating at the same temperature. Thus, a 150°C reduction in the synthesis temperature for cordierite

was successfully accomplished via intensive grinding of the powder raw materials. The mechanochemical technique, therefore, led to a decrease in the synthesis temperature for cordierite.

Table 5.3. Analysis of Variance for the cordierite synthesis rate experiment in A and C.

Source	Sum of Squares	Degrees of freedom	Mean Square	F Value	Prob > F
Model	3894.64	6	649.11	402.92	0.0381
A	111.53	1	111.53	69.23	0.0761
C	2653.93	1	2653.93	1647.36	0.0157
AB	644.94	1	644.94	400.33	0.0318
AC	145.44	1	145.44	90.28	0.0668
BC	7.66	1	7.66	4.76	0.2737
ABC	331.15	1	331.15	205.55	0.0443
Residual	1.61	1	1.61		
Cor Total	3896.25	7			

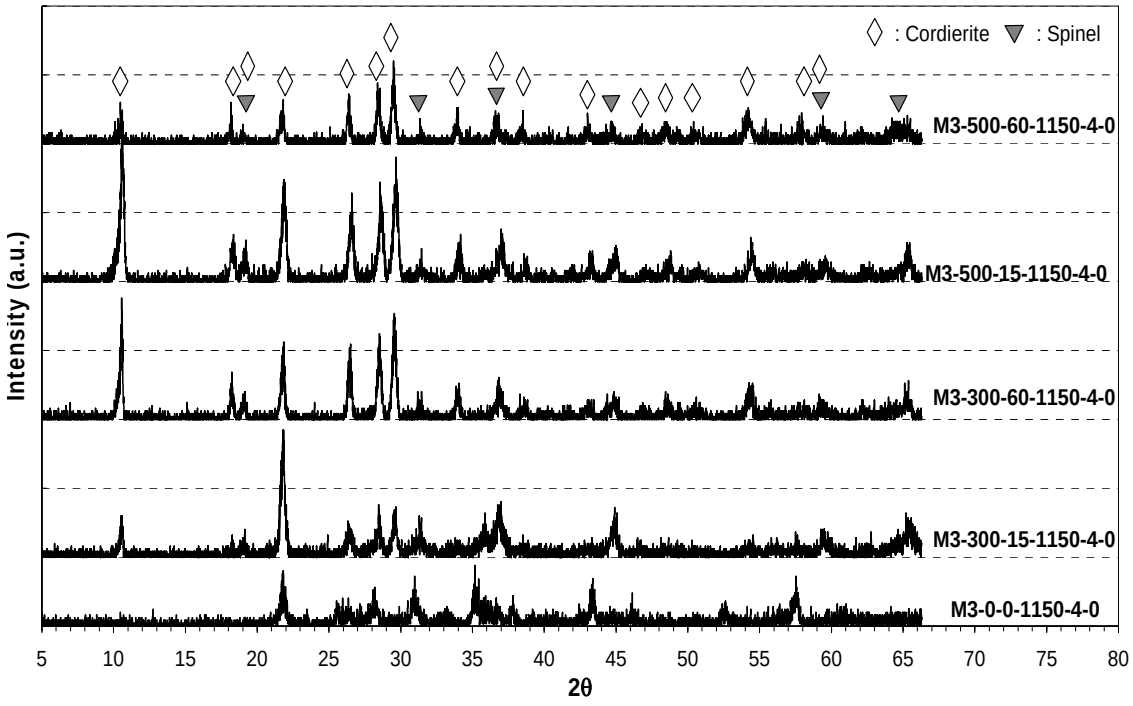

Figure 5.12. XRD patterns of the ground M3 samples that were heated at 1150^{o}C.

5.2.2.2. Effect of Additives on Cordierite Synthesis

Having accomplished a reduction in the required temperature for cordierite synthesis, efforts were directed at further reductions by the use of additives like magnesium borate. In this study, magnesium borate ($2MgO.B_2O_3$) was synthesized in-house to be used as an additive to accelerate phase-transformation kinetics and to improve bulk density. The XRD pattern of synthesized magnesium borate is illustrated in Figure 5.13. All peaks in the pattern were a perfect match with magnesium borate. Relatively broad peaks were observed and are thought to result from fine crystallite size of synthesized magnesium borate.

Effect of the amount of additives on the cordierite synthesis was investigated at different heat treatment temperatures and soak times. M1 mixture (Table 4.3) was selected as the basis for this part of the study. 2 and 5 wt% magnesium borate was added to the M1 mixture. These specimens were heated at 1100°C and 1200°C for 1hr and 1100°C for 4 hrs. These XRD patterns are shown in Figures 5.14-16, respectively.

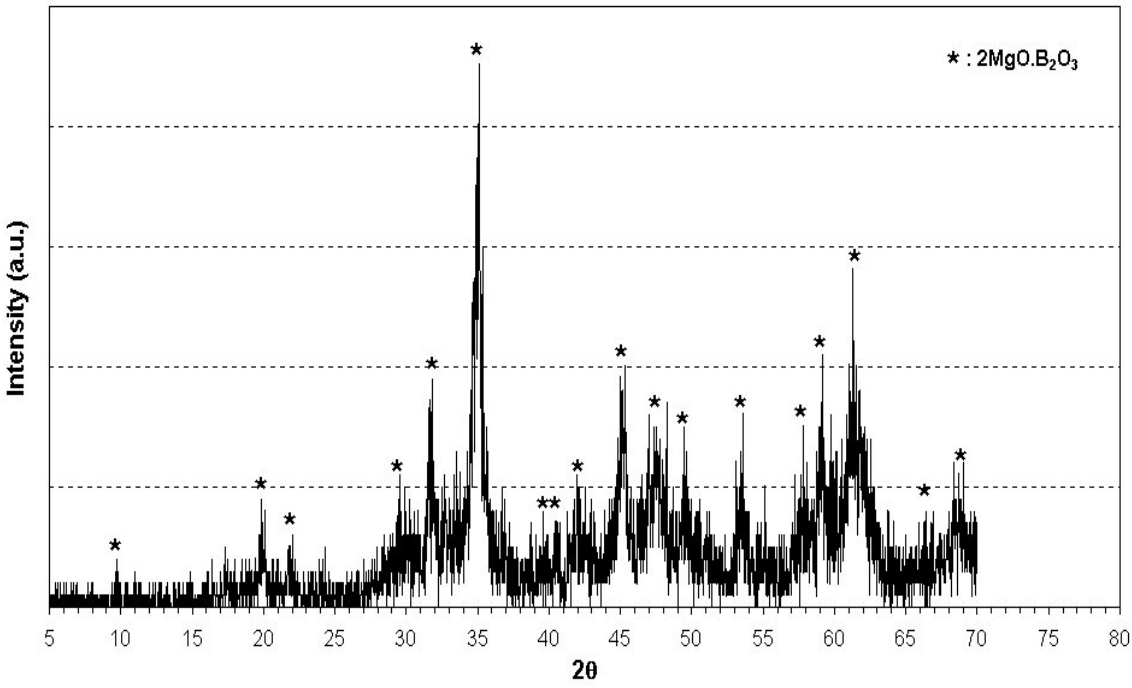

Figure 5.13. XRD pattern of synthesized magnesium borate.

The raw materials (in Figure 5.14) again did not react with each other completely at 1100°C for 1 hr like the original M mixtures that were fired at 1200°C for

1hr (Figure 5.5). Corundum, cristobalite, spinel and magnesium silicate were detected in the XRD patterns. We observed that additive did not decrease the synthesis temperature for samples heated at 1100°C for 1hr. However, when the specimens were heated at 1200°C for 1hr, cordierite was synthesized on the 2 and 5 wt% additive mixtures. Their XRD patterns are shown in Figure 5.15. In addition to cordierite phase, small amount of spinel phase was also detected in these XRD patterns.

We also investigated the effect of soak time on cordierite synthesis. The M1 specimens with 2 and 5 wt% additives were again heated at 1100°C but this time for 4 hrs. The results are shown in Figure 5.16. Cordierite phase was this time observed only for 5 wt % of additive mixture. Small amounts of spinel and mullite phases were also observed in this sample. Soak time was therefore another significant factor in cordierite synthesis.

According to these results, in addition to mechanochemical treatment, firing temperature and soak time, the percentage of additives is another important parameter for cordierite synthesis.

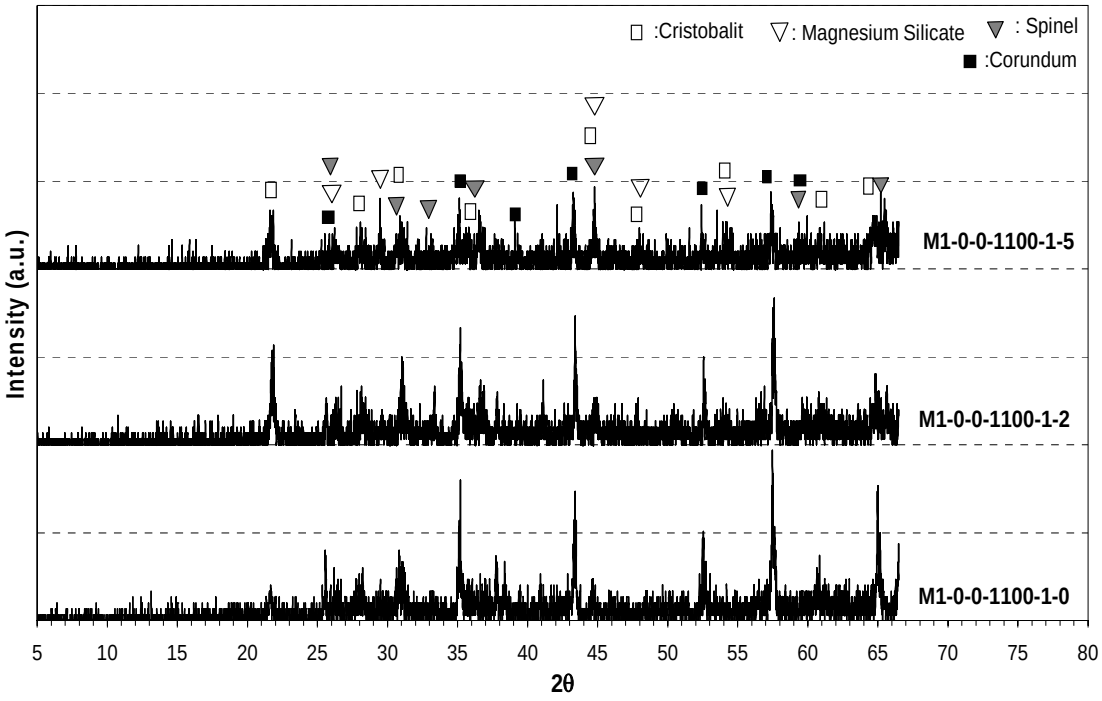

Figure 5.14. XRD patterns of the M1 samples with/without additives that were heated at 1100°C.

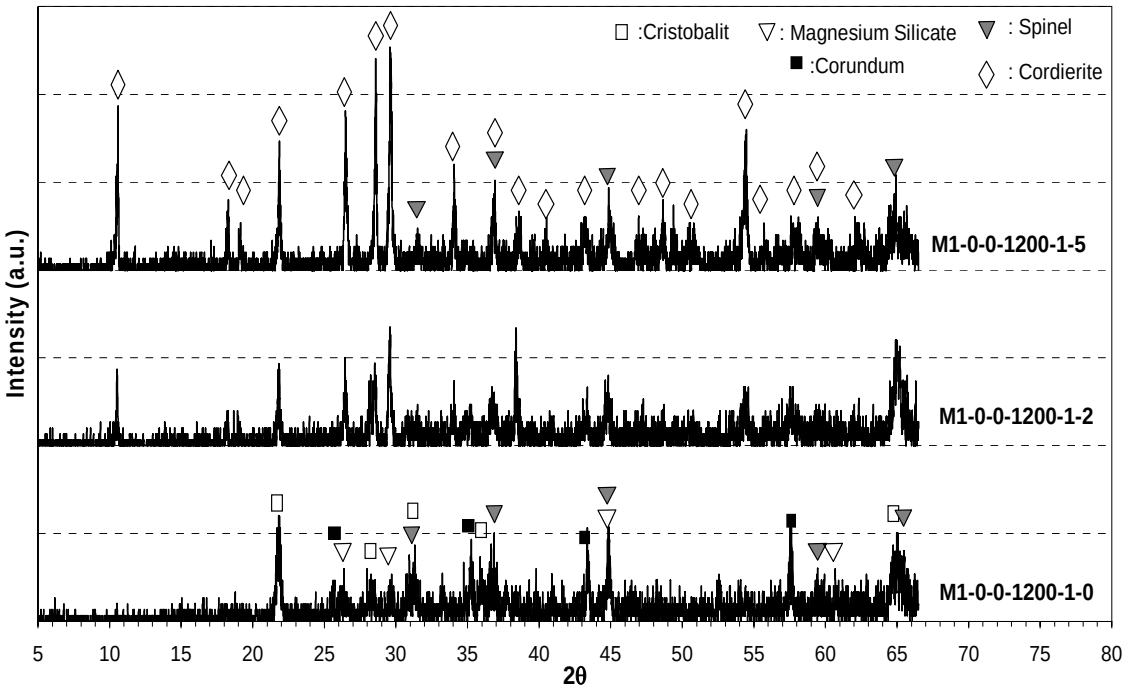

Figure 5.15. XRD patterns of the M1 samples with/without additives that were heated at 1200^{o}C.

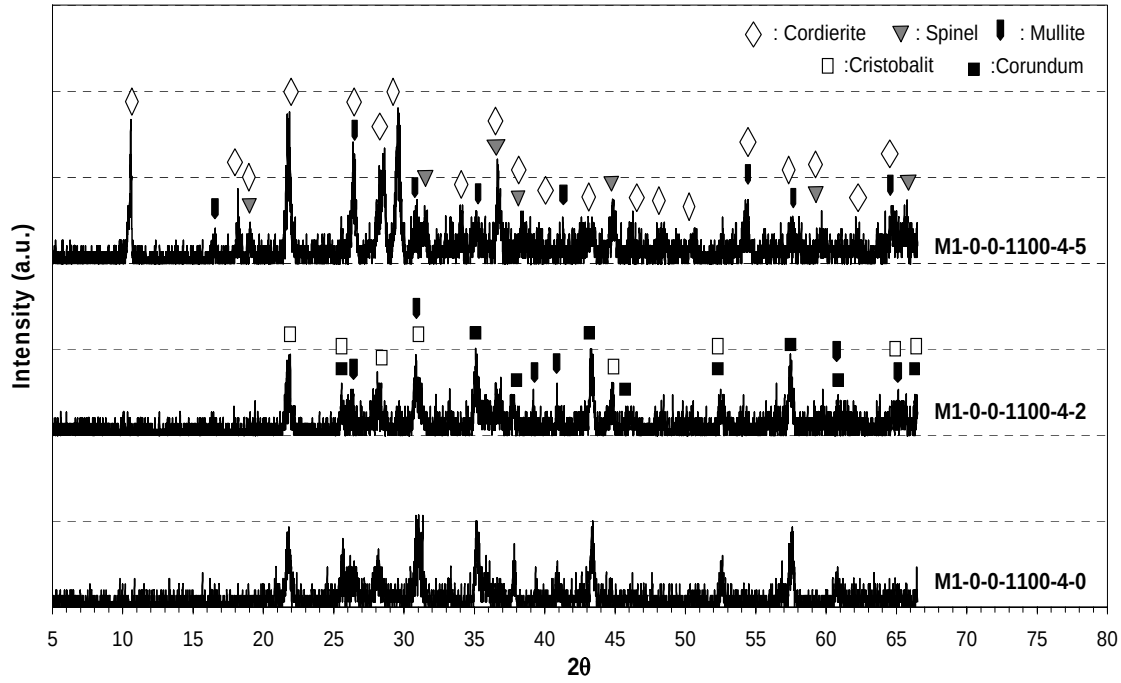

Figure 5.16. XRD patterns of the M1 samples with/without additives that were heated at 1100^{o}C for 4 hrs.

5.2.2.3. Effect of Grinding and Additives on the Cordierite Synthesis

In this part of the study, the combined effect of grinding and additives was investigated on cordierite synthesis.

Initially M3 mixture was mixed with 5 wt% magnesium borate and without intensive grinding was heated at different temperatures for 4 hrs. The purpose was to compare the effect of grinding on heated mixtures. The results are shown in Figure 5.17. The cordierite was synthesized at nearly 1100°C. But small amount of spinel and mullite phase was also detected.

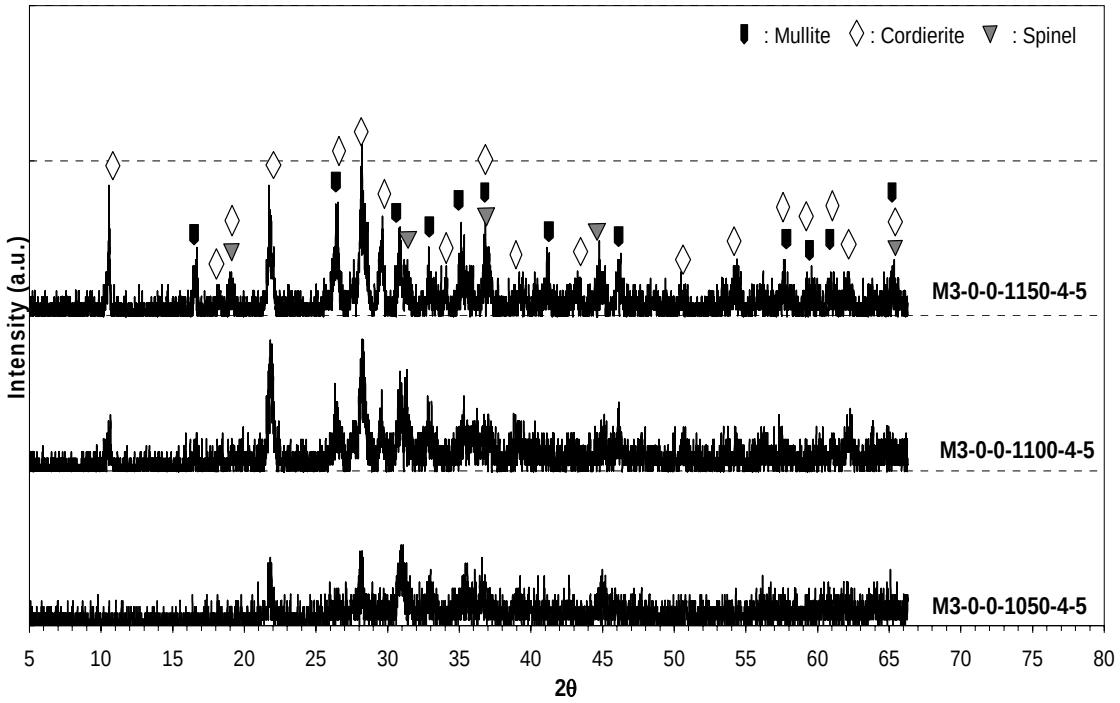

Figure 5.17. XRD patterns of the M3 samples with 5 wt % additive that were heated at different temperatures.

To compare the combination of grinding and additive effect on the cordierite synthesis temperature, the M3 mixture with 5 wt% magnesium borate was ground at 300 rpm for 60 min. The ground mixture was compacted and fired at 1000, 1050, 1100 and 1150°C for 4 hrs. The x-ray diffraction patterns of heat treated specimens are shown in Figure 5.18.

According to the XRD patterns, cordierite synthesis temperature was decreased down to nearly 1000°C. The use of longer soak times at that temperature may lead to

further reductions in synthesis temperature but longer soak durations were not tested in this project. These results show that cordierite synthesis temperature was decreased nearly by 250°C via the use of additives and mechanochemical synthesis.

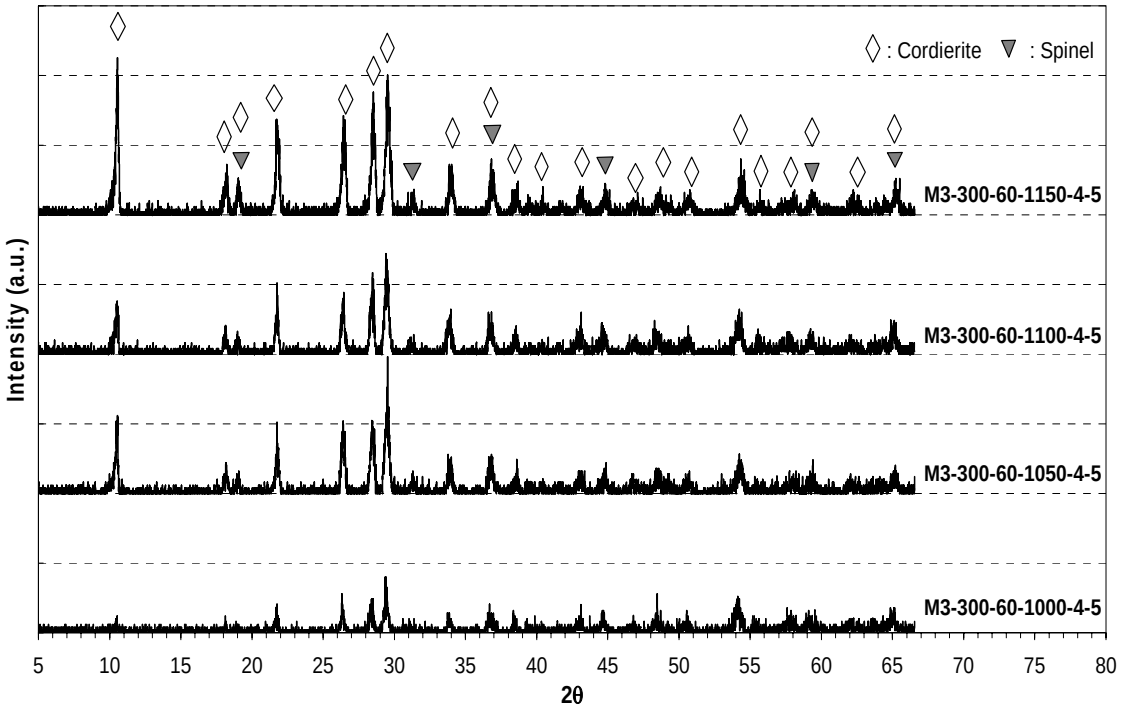

Figure 5.18. XRD patterns of the ground M3 samples with 5 wt% additive that were heated at different temperatures.

5.2.3. Differential Thermal Analyses (DTA)

The results of DTA measurement for ground and unground M3 mixtures are shown in Figure 5.19. The same intermediate step of the gibbsite dehydration peak (See Fig. 5.3) at nearly 250°C is also observed in the unground M3 mixture. The endothermic peak at 290°C show dehydration of aluminum hydroxide. The peak was shifted to lower temperature, when grinding time and speed were increased. The endothermic peak intensity also decreased on further grinding. These were attributed to the destruction of crystal structure as a result of extensive grinding, and local increases in temperature during grinding.

The small endothermic peak observed in M3-0-0-0-0-0 mixture at 520°C corresponded to kaolinite dehydroxylation. This peak was very weak and again shifted to lower temperatures with increasing grinding times.

The M3-0-0-0-0-0 sample also present a small endothermic peak at 960°C, corresponding to the talc dehydroxylation and its transformation to enstatite [19]. The samples that were mechanochemically treated showed a disordered phase whose decomposition is easier and took place at comparatively lower temperatures.

A small exothermic peak at 1000°C was observed in the M3 sample This peak is due to the transformation of the non-crystalline structure of the kaolinite into a spinel or premullite phase. This peak appeared at 940°C in the M3-500-15-0-0-0 mixture. This peak is also observed in the further ground mixtures M3-300-60-0-0-0 and M3-500-60-0-0-0. The intensity of this peak slightly increased in the A3 mixture. However, there are no important variations in the peak temperature positions.

To investigate the effect of additives and grinding on cordierite synthesis, prepared samples were also characterised by DTA method. Their DTA results are shown in Figure 5.20. There was no significant change from the original M3-0-0-0-0-0 mixture (see fig 5.19) and the M3-0-0-0-0-5. However, there was a strong exothermic peak at 1100°C in the mixtures with additives (Fig 5.20). This peak corresponded to the crystallization of α-cordierite.

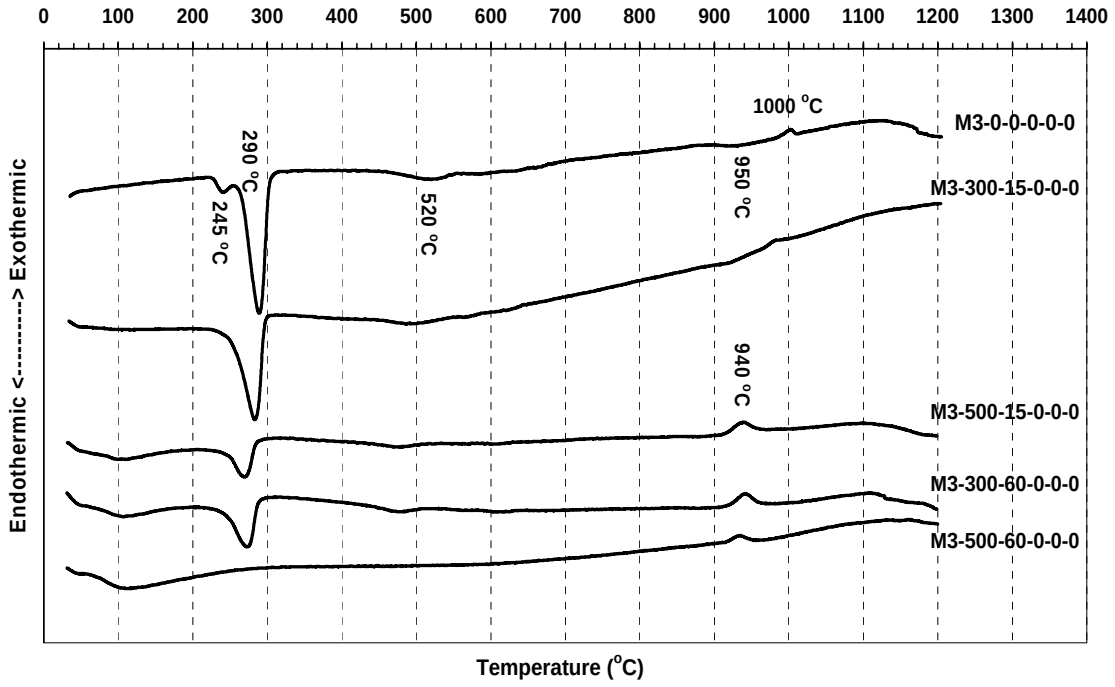

Figure 5.19. DTA analysis of ground and unground mixtures.

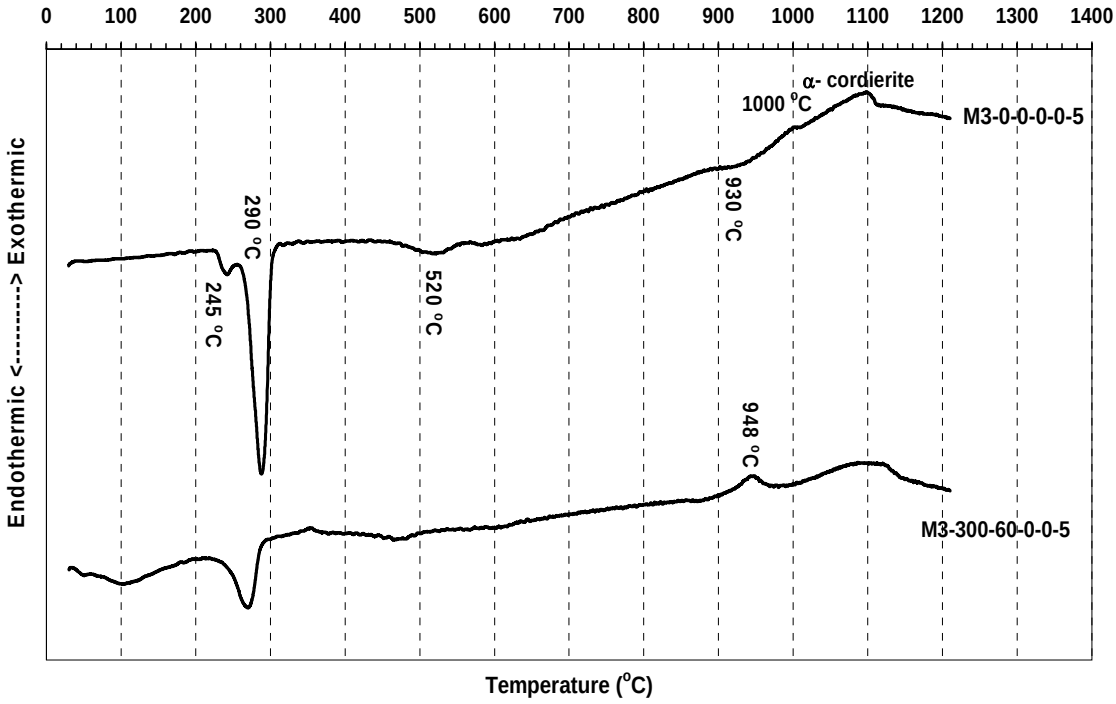

Figure 5.20. DTA analysis of ground and unground M3 samples with 5 wt% additive.

5.2.4. Microstructural Analyses (SEM)

In order to investigate the effect of grinding on particle size and morphology of cordierite mixtures, SEM analyses were performed. Figure 5.21 illustrates secondary electron images of selected powder samples. Significant particle size reduction was achieved after 15 min of grinding at 300 rpm (Figure 5.21-b) when compared to unground powder mixture (Figure 5.21-a). Further reduction occurred at 15 and 60 min of grinding at 500 rpm (Figure 5.21-c and d). Due to the fine particle size, the powders tended to form agglomerates. Some of the raw material particles like talc were plate-like before grinding. After grinding, on the other hand, all particles were round shaped.

Effect of grinding and additive use on microstructure of cordierite were inspected by using SEM. Backscatter electron images (BSE) of polished sections of selected samples which were produced by grinding at 300 rpm for 60 min and followed by heating at 1150^{o}C for 4 hrs are shown in Figure 5.22. One of the samples contained 5 wt% of magnesium borate (Figure 5.22-b). Angular and needle-like light grey areas were observed in the sample with no additive. Such areas were analyzed by EDS and were found to contain a higher proportion of alumina (Figure 5.22-a). However, such an alumina-rich phase was not detected in the sample with additive.

Both samples displayed bi-model pore size distribution including 1-2 μm and 5-20 μm pores. The proportion of fine pores (1-2 μm) was significantly reduced in the sample with 5 wt% $2MgO.B_2O_3$ additive (Fig. 5.22-b) compared to the sample without additive (Fig 5.22-a). Pores were angular in the first sample, on the other hand they were rounded in the latter. This effect probably originated from better diffiusion in the sample with additives.

Density and porosity measurements of heated pellets were also conducted for all samples for cordierite synthesis. These results are given in Appendix A.

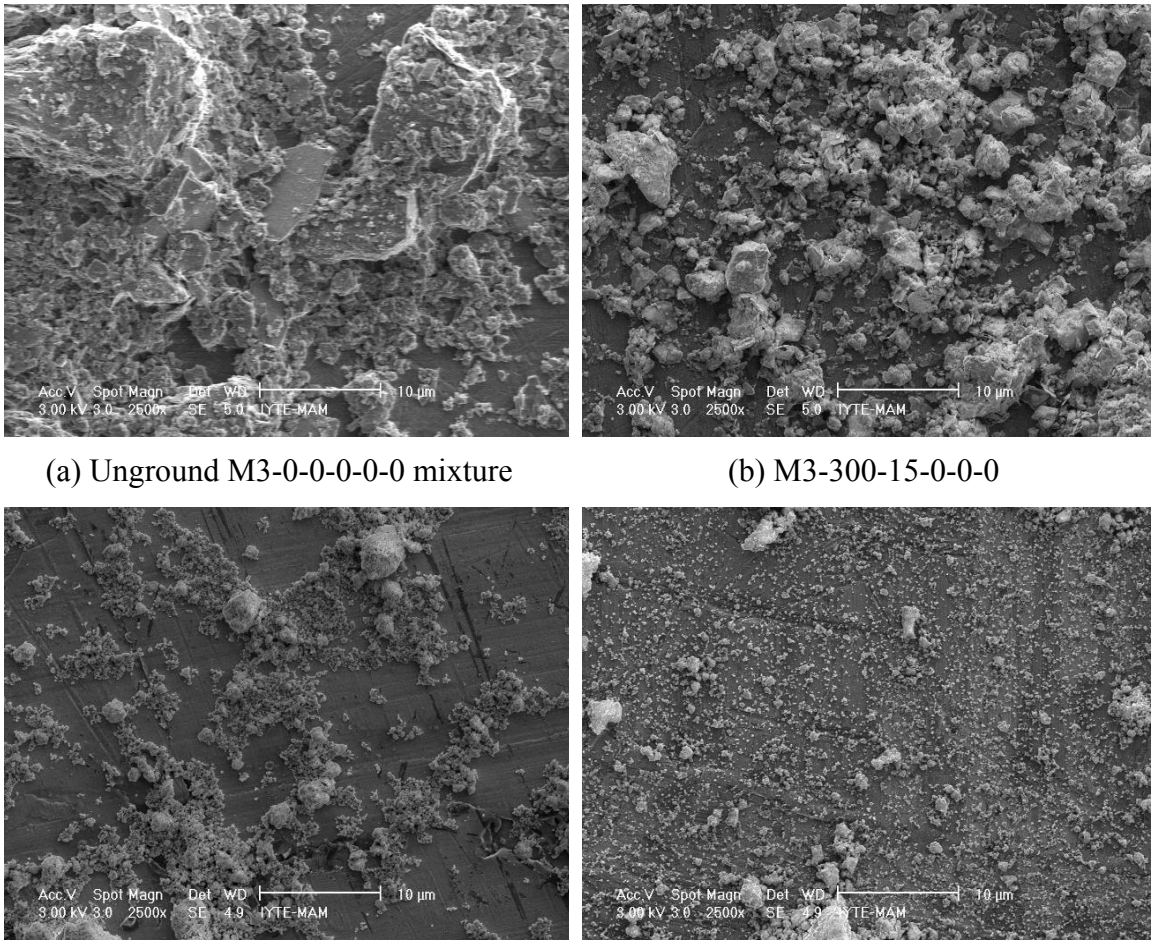

(a) Unground M3-0-0-0-0-0 mixture (b) M3-300-15-0-0-0

(c) M3-500-15-0-0-0 (d) M3-500-60-0-0-0

Figure 5.21. SEM micrographs of powder specimens ground at different rotational speeds and grinding times.

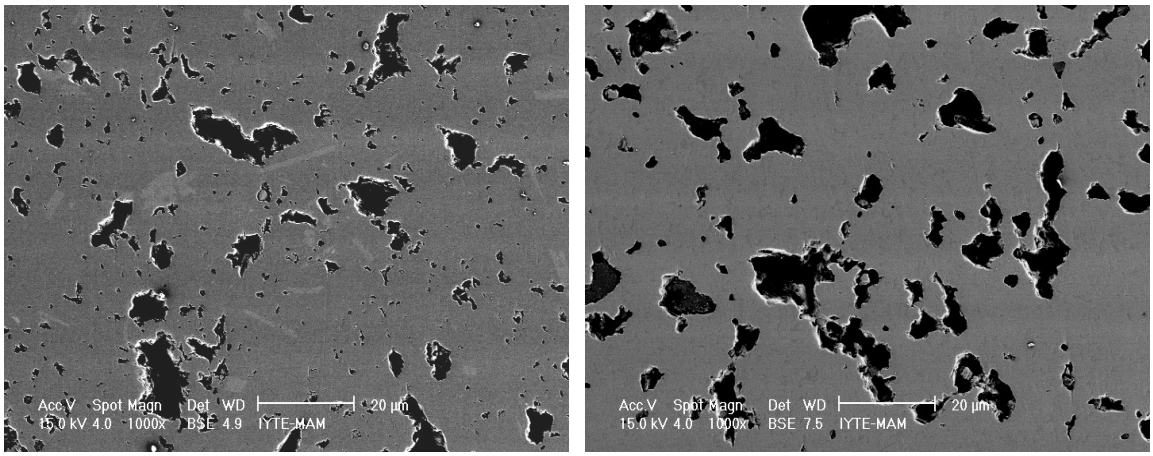

a) M3-300-60-1150-4-0 b) M3-300-60-1150-4-5

Figure 5.22. Comparison of additive effect on the cordierite microstructure.

5.2.5. FTIR Spectroscopy

Effect of grinding on the raw materials was also investigated by FTIR analyses. FTIR patterns of as mixed M3-0-0-0-0-0 and ground M3 mixtures are shown in Figure 5.23.

The crystal structure of gibbsite contains six unique OH groups so six unique OH stretching [*v*(OH)] bands are expected to occur in IR spectra of gibbsite. However, only five *v*(OH) bands have been observed [43]. The sixth *v*(OH) band in the IR spectrum of gibbsite was observed by the use of low-temperature IR spectroscopy. This technique narrows the linewidths of the *v*(OH) bands and thereby improve the resolution. At ambient temperature (300 K), five IR bands are resolved at 3621, 3627, 3463, 3395, and 3376 cm^{-1}. At low temperature (12 K), six bands are resolved at 3619, 3523, 3509, 3456, 3385, and 3361 cm^{-1} [44].

Our band positions in M3-300-15-0-0-0 (Fig 5.23.); 3627, 3533, 3473 and 3400 cm^{-1} is in agreement with the values in the literature. However, 3395, and 3376 cm^{-1} bands are not well resolved so they are observed as a single OH band at 3400 cm^{-1}. The sixth band can not be resolved in our experimental conditions (12 K).

The kaolin Al-OH stretching bands are resolved at 3622, 3651 and 3697 cm^{-1} [45]. Our results are in agreement with the previous study and our kaolin sample's Al-OH stretching bands are at 3625 and 3700 cm^{-1} (in Fig 5.23, sample M3-300-15-0-0-0). However, the 3651 cm^{-1} Al-OH stretching band is not resolved in our samples. After grinding, the kaolinite structure transformed into metakaolinite form and their IR

spectrum also changed. When grinding increases the IR spectrum of metakaolinite shows absorption band at 3460 and 1660 cm^{-1}. These bands are assigned as absorbed water. The Al-OH strecthing bands at 3625 and 3700 cm^{-1} disappear on grinding.

Grinding also causes the absoption bands at 918, and 1024 cm^{-1} to merge into one broad band, reflecting the amorphisation of the crystalline structure. The bands at 470, 761, 918 and 1024 cm^{-1} are assigned as strecthing and bending vibrations of SiO_4 tetrahedra.

In the literature, talc Si–O vibration band was observed at 1027 cm^{-1} [46]. The presence in all spectra (except M3-500-60-0-0-0 sample) of a band located at 3676 cm^{-1} is related to the O–H stretching vibration for talc. Grinding causes the Si-O stretching band at 900-1200 cm^{-1} and the bending vibration at 400-600 cm^{-1} to broaden, with the additional appearance of water vibrations at 1660 cm^{-1} and 3400-3500 cm^{-1}, possibly reflects an increased tendency of the mechanically activated material to hydrate in the presence of atmospheric water [47].

To investigate the structural changes that occurred towards the formation of cordierite through different phase transitions of the powder M3-300-60-1200-4-0 FTIR studies were performed in the wavenumber range 4600-400 cm^{-1}; however, the spectra in the wavenumber region 1600-400 cm^{-1} are presented for this sample in Figure 5.24.

A characteristic strongest band in region 900-1000 cm^{-1} appeared in the M3-300-60-1200-4-0 sample, which corresponded to the presence of Si-O-Si asymmetric stretching vibration. The band between 1100 and 1400 cm^{-1} indicated the character of symmetric stretching of AlO_4 tetrahedra. The band at around 770 cm^{-1} for the sample was due to symmetric stretching mode of the Si-O-Si bond. The bands that appeared around 580 and 480 cm^{-1} assigned to the Al-O stretching vibration in isolated AlO_6 octahedra [48].

The characteristic peaks of α-cordierite were found at around 1185, 912, 950, 770, 680, 620, 580, 480 and 425 cm^{-1} for the sample M3-300-60-1200-4-0 [49].

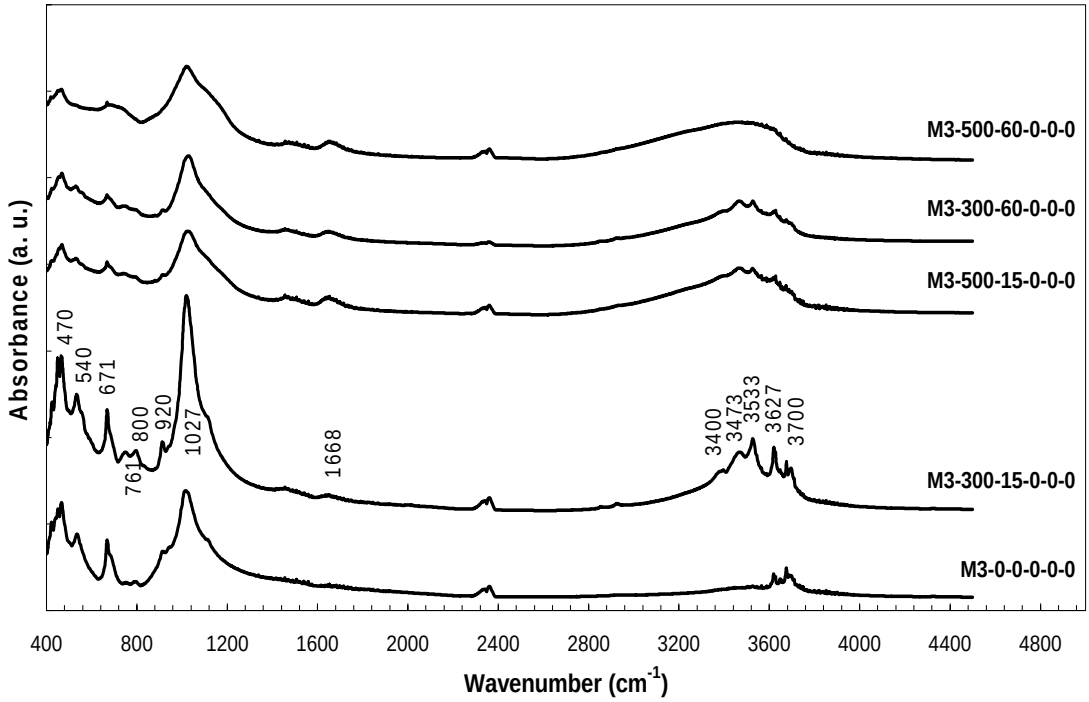

Figure 5.23. FTIR patterns of the as mixed and ground M3 mixtures.

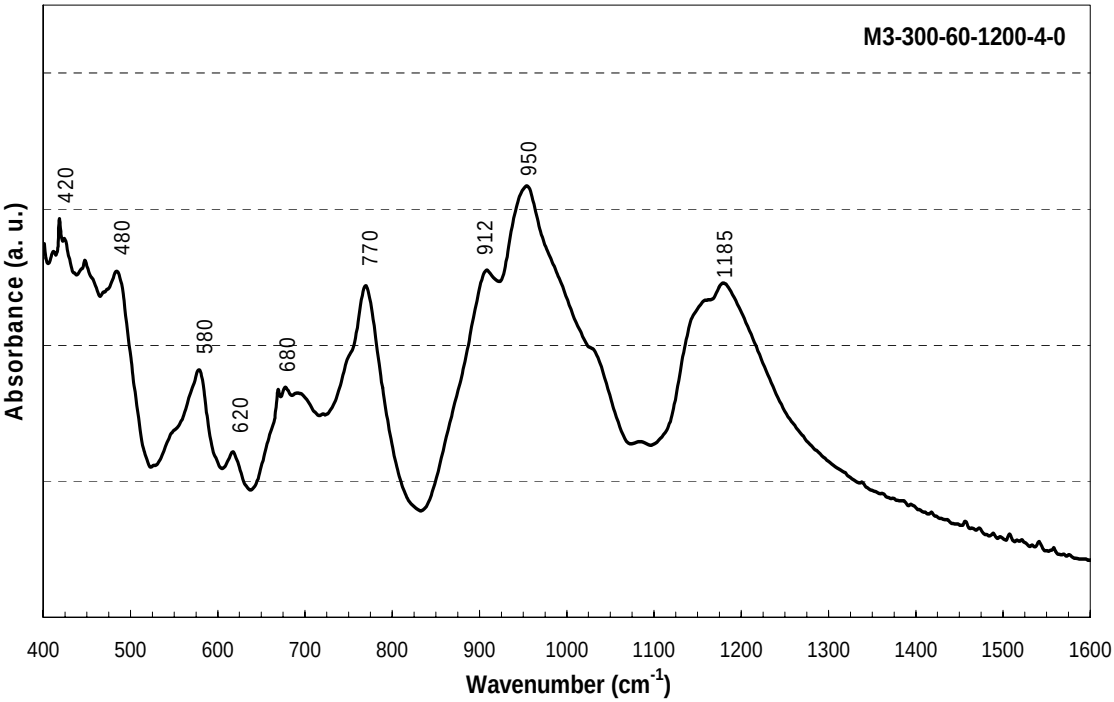

Figure 5.24. FTIR spectra of the powder sample M3-300-60-1200-4-0.

CHAPTER 6

CONCLUSIONS

In this study, synthesis of spinel and cordierite ceramics were investigated by using mechanochemical technique. The advantages of this type of synthesis over the conventional solid state reaction were demonstrated. The syntheses temperatures of the ceramics were gradually decreased by mechanochemical technique. This simple stage and ecologically safe (no solvent or intermediate heating) method was performed and its parameters such as grinding speed and grinding time were examined on the cordierite synthesis. In addition to the mechanochemical technique, the effect of additive use and the combined effect of additive use and grinding on cordierite synthesis were also studied.

The powder amorphization and syntheses were tracked by X-ray diffraction and DTA methods. The particle size and morphology of powders and synthesized crystals were observed by SEM. The bonding structure of ground mixture and synthesized cordierite crystals were investigated by FTIR.

In the first part of the study, spinel synthesis was investigated and synthesis of spinel powder was achieved at low temperature by the use of mechanochemical technique. After 50 minutes of grinding, amorphization of the starting materials was completed. Partial growth of spinel crystals in XRD patterns was detected after 110 minutes of grinding without heating. Heating of samples ground for 60 minutes produced spinel crystals at temperatures less than $1000^{o}C$.

In the second part, cordierite synthesis was studied. Suitable type of mixtures with different molar ratio (1:1:2 or 2:2:5) and different alumina sources (Al_2O_3 or $Al(OH)_3$) were examined for cordierite synthesis. 1:1:2 molar ratio and $Al(OH)_3$ use as alumina source showed better result than the other combinations and cordierite ceramic was synthesized at $1300^{o}C$ by conventional solid state reaction by using these parameters.

Mechanochemical synthesis of cordierite was investigated by experimental design methodology to draw more clear and objective conclusions from the data. The single replicate of 2^3 full factorial design was generated. In these experiments, grinding speed, grinding time and heating temperature were chosen as the parameters influencing

the cordierite synthesis. The results of the statistically designed experiments showed that heating temperature was the main parameter for the synthesis. This was an expected result. Another significant finding of the statistical analysis was that there was an interaction between grinding time and grinding speed.

Cordierite is generally synthesized at 1300^{o}C by conventional solid state reaction. On the contrary, cordierite was synthesized at 1150^{o}C by mechanochemical technique in this study. As a result, the synthesis temperature of cordierite was decreased nearly by 150^{o}C.

In order to further decrease the synthesis temperature of cordierite, magnesium borate ($2MgO.B_2O_3$) was synthesized in-house and it was used as an additive. 2 and 5 wt% magnesium borate was added to the M1-0-0-0-0-0 mixture. This additive accelerated phase-transformation kinetics and cordierite was synthesized at 1100^{o}C by adding 5 wt% of magnesium borate. This has led to further decreases in cordierite synthesis temperature to a total reduction by 200^{o}C.

The combined effect of grinding and additive use was investigated on cordierite synthesis. 5 wt% magnesium borate was added to M3 mixture and the mixture was ground at 300 rpm for 60 min. According to the XRD patterns, cordierite synthesis temperature was decreased down to nearly 1000^{o}C. These results showed that cordierite synthesis temperature was decreased nearly by 250^{o}C via the use of additive and mechanochemical synthesis simultaneously.

Further work for spinel may include testing of mechanical and thermal properties of the powder for potential use in, for example, refractories industry. Mechanical properties of synthesized cordierite ceramics may be studied. Ground cordierite mixtures can be extruded into honeycomb substrates and firing temperature, porosity, thermal shock resistance and mechanical strength of these substrates can be investigated.

REFERENCES

[1] S.J. Zinkle, C. Kinoshita, *J. Nucl. Mater*. **251** (1997) 200.

[2] E. Kostic, S. Kiss, S. Boskovic, S. Zec., "Mechanical activation of the gamma to alpha transition in Al_2O_3", *Powder Technology*, **91** (1997), 49-54.

[3] Y.M. Chiang, D. P. Brinie III and W. D. Kingery., "Physical Ceramics", John Wiley&Sons Inc. New York, (1997).

[4] Ursuka Steinike and Klara Tkacova, "Mechanochemistry of Solids-Real Structure and Reactivity", *J. Materials Synthesis and Processing*, **8** [3/4], (2000), 197-203.

[5] V.V. Boldyrev and K. Tkacova, "Mechanochemistry of Solids: Past, Present and Prospects", *J. Materials Synthesis and Processing*, **8** [3/4] (2000), 121-132.

[6] E. Ivanov and C. Suryanarayana, "Materials and Process Design through Mechanochemical Routes", *J. Materials Synthesis and Processing*, **8** [3/4], (2000), 235-244.

[7] P. Balaz, "Extractive Metallurgy of Activated Minerals", Elsevier, Amsterdam, (2000).

[8] Zaluska, L. Zaluski, and J. O. Ström-Olsen, *J. Alloys Comp*. **288**, 217 (1998).

[9] L. Bobet, C. Even, Y. Nakamura, E. Akiba, and B. Darriet, *J. Alloys Comp*. **298**, 279 (2000).

[10] F.A. Costa Oliveira, and C.J. Fernandes, "Mechanical and thermal behaviour of cordierite-zirconia composites", *Ceramics International*, **28**, (2002), 79-91.

[11] M. D. Karkhanavala and F. A. Hummel, "The Polymorphism of Cordierite", *J. Am. Ceram. Soc.* **36** [12], (1953), 389-392.

[12] S.H. Knickerbocker, A.H. Kumar, L.W. Herron, "Cordierite glass-ceramics for multilayer ceramic packing", *American Ceramic Society Bulletin* **72** [1] (1993), 90-95.

[13] S. Mei, J. Yang, J. M. F. Ferreira., "Cordierite-based glass-ceramics processed by slip casting", *J. European Ceramic Society*, **21** (2001), 185-193.

[14] K. Sumi, Y. Kobayashi, E. Kato., "Low-Temperature fabrication of cordierite ceramics from kaolinite and magnesium hydroxide mixtures with Boron Oxide Additions", *J. Am. Ceram. Soc*. **82** [3], (1999), 783-85.

[15] Ö. Çakır, "Production of Cordierite from Domestic Raw Materials" M. Sc. Thesis, June 1981, Middle East Technical University, Ankara.

[16] S.T. Sevinçtav, and M., Marşoğlu, "Kordiyerit Sentezi ve Katalitik Konverter Altlık Şekillendirme", V. Ceramics Congress With International Participations/TÜRKİYE, (2001), 318-324.

[17] M. Awano, H. Takagi, Y. Kuwahara., "Grinding Effects on the Synthesis and Sintering of Cordierite", *J. Am. Ceram. Soc*. **75** [9], (1992), 2535-40.

[18] S. Kurama, N. Ay, "Effect of Grinding Time and MgO Source on Cordierite Formation", *Am. Ceram. Soc. Bul*. **81** [11] (2002), 58-61.

[19] S. Tamborenea, A.D. Mazzoni and E.F. Aglietti, "Mechanochemical activation of minerals on the cordierite synthesis", *Thermochimica Acta*, **411** (2004), 219-224.

[20] M. L. Keith and J. F. Schairer, "The satability field of sapphirine in the system MgO-Al_2O_3-SiO_2", *Journal of Geol*., **60**, (1952), 181-186.

[21] Kingery, Bowen H., Uhlmann D.R., "Introduction to Ceramics", John Wiley&Sons Inc. New York, (1976).

[22] William E. Lee and W. Mark Rainforth, "Ceramic Microstructures property control by processing", Chapman & Hall, London, (1994), 44,45.

[23] Jenn-Ming Wu and Shiang-Po Hwang "Effects of (B_2O_3, P_2O_5) Additives on Microstructural Development and Phase-Transformation Kinetics of Stoichiometric Cordierite Glasses" *J. Am. Ceram. Soc.* **83** [5], (2000), 1259-65.

[24] S. Kurama, E. Özel and N. Ay, "Düşük Sıcaklıkta Kordierite Üretime", 10. National Clay Symposium, Konya/TÜRKİYE, (2001), 524-531.

[25] P. Bartha, H.J. Klischat., "Present State of the Refractory Lining for Cement Kilns", *CN-Refractories*, **6** [3], (1999).

[26] Cemail Aksel, Brian Rand, Frank L. Riley, Paul D. Warren, "Mechanical properties of magnesia-spinel composites", *Journal of the European Ceramic Society* **22** (2002), 745–754.

[27] R. Sarkar, S.K. Das, G. Banerjee., "Calcination effect on magnesium hydroxide for the development of magnesium aluminate spinel", *Ceramics International*, **26** (2000), 25-28.

[28] H. Reveron, D. G. Campos, R. M. Rodriguez, J. C. Bonassin., "Chemical synthesis and thermal evolution of $MgAl_2O_4$ spinel precursor prepared from industrial gibbsite and magnesia powder", *Materials Letters*, **56**, [1-2] (2002), 97-101.

[29] V. K. Singh, R. K. Sinha., "Low temperature synthesis of spinel ($MgAl_2O_4$)", *Materials Letters*, **31** (1997), 281-285.

[30] L.R. Ping, A.M. Azad, T.W. Dung., "Magnesium aluminate ($MgAl_2O_4$) spinel produced via self-heat-sustained (SHS) technique", *Materials Research Bulletin*, **36** (2001), 1417-1430.

[31] D.M. Roy, R. Roy, E.F. Orbon, *J. Am. Ceram. Soc*. **25**, (1953), 337-361.

[32] A. Mazzoni, E.F. Aglietti and E.Pereira., "Preparation of spinel powders ($MgAl_2O_4$) at low temperature by mechanical activation of hydroxide mixtures", *Latin American Research*, **21** (1991), 63-68.

[33] E. Kostic, S. Kiss, S. Boskovic., "Decrease of the $MgAl_2O_4$ formation temperature", *Powder Technology*, **92** (1997), 271-274.

[34] W. Kim, F. Saito., "Effect of grinding on synthesis of $MgAl_2O_4$ spinel from a powder mixture of $Mg(OH)_2$ and $Al(OH)_3$", *Powder Technology*, **113** (2000), 109-113.

[35] B. Plesingerova, N. Stevulova, M. Luxova and E. Boldizarova., "Mechanochemical Synthesis of Magnesium Aluminate Spinel in Oxide-Hydroxide Systems", *Journal of Materials Synthesis and Processing*, **8**, [5/6], (2000), 287-293.

[36] M. S. Kırıkoğlu, A. Sümer, S. G. Özkan, and G. Özden, "Investigation of Some Physical and Chemical Properties With Respect to Processing of Kaolin Samples from Sivas Deposits in Turkey", *Key Engineering Materials*, **264-268**, (2004), 1423-1426.

[37] Omya Madencilik A.Ş., Product information "Egyptian Talc Et 5", İstanbul, (2004).

[38] Alcoa Industrial Chemicals Europe, "Calcined and Reactive Aluminas for the Ceramic Industry Product Data", Frankfurt, (2001).

[39] H. Harris and W. Lautenberger, "Strategy of experimentation", E.I. Dupont Short Course Notes, (1976).

[40] Standard Test Methods for Apparent Porosity, Water Absoption, Apparent Specific Gravity, and Bulk Density of Burned Refractory Brick and Shapes by Boiling Water, ASTM Designation: C20-87, Annual Book of ASTM Standards, Vol., (1987).

[41] E. Yalamaç, S. Akkurt, M. Çiftçioğlu. "Low Temperature Synthesis of Spinel Powders by Mechanical Grinding", *Key Engineering Materials*, **264-268**, (2004), 53-56.

[42] W.C. Mohr "Development of properties in cordierite Kiln Furniture" *American Ceramic Society Bulletin* **56** (1977), 428-430.

[43] R.L. Frost, J.T. Kloprogge, S.C. Russell, and J.L. Szetu, "Vibrational spectroscopy and dehydroxylation of aluminum (oxo)hydroxides: Gibbsite", *Applied Spectroscopy*, **53**, (1999), 423–434.

[44] S. Wang and C.T. Johnston, "Assignment of the structural OH stretching bands of gibbsite", *American Mineralogist*, **85**, (2000), 739-744.

[45] J. Temuujın, G. Burmaa and J. Amgalan, "Preparation of Porous Silica from Mechanically Activated Kaolinite", *Journal of Porous Materials,* **8**, (2001), 233–238.

[46] Wilkins R.W.T. and Ito J., "Infrared spectra of some synthetic talcs". *American Mineralogist* , **52**, (1967) 1649-1661.

[47] J. Temuujin, K. Okada, TS. Jadambaa, K. J. D. Mackenzie, and J. Amarsanaa, "Effect of grinding on the preparation of porous material from talc by selective leaching" *Journal of Materials Science Letters* **21**, (2002), 1607 – 1609.

[48] M.K. Naskar and M.Chatterjee, " A novel process for the synthesis of cordierite powders from rice husk ash and other sources of silica and their comparative study", *J. European Ceramic Society*, **24,** (2004), 3499-3508.

[49] FDM Electronic Handbook software program, http://www.fdmspectra.com/ehb_registration.htm.

APPENDIX A

Archimedes Density of Cordierite Mixture Pellets

		Apperent Porosity, %	Water Absorbtion, %	Bulk Density, g/cm^3	Theoretical Density, %
1	M1-0-0-1200-1-0	35.554	18.152	1.959	73.91
2	M2-0-0-1200-1-0	33.475	17.031	1.966	74.17
3	M3-0-0-1200-1-0	41.537	24.280	1.711	64.56
4	M4-0-0-1200-1-0	37.120	20.684	1.795	67.72
5	M1-0-0-1300-1-0	28.096	14.102	1.992	75.18
6	M2-0-0-1300-1-0	27.139	13.939	1.947	73.47
7	M3-0-0-1300-1-0	36.692	21.128	1.737	65.54
8	M4-0-0-1300-1-0	32.025	17.741	1.805	68.12
9	M3-300-15-1100-4-0	39.118	21.770	1.797	67.81
10	M3-300-60-1100-4-0	10.646	4.455	2.390	90.17
11	M3-500-15-1100-4-0	17.281	7.626	2.266	85.51
12	M3-500-60-1100-4-0	17.238	8.104	2.127	80.27
13	M3-300-15-1200-4-0	34.219	18.975	1.803	68.05
14	M3-300-60-1200-4-0	6.866	2.932	2.342	88.37
15	M3-500-15-1200-4-0	8.671	3.875	2.238	84.45
16	M3-500-60-1200-4-0	25.192	13.144	1.917	72.32
17	M3-0-0-1150-4-0	39.594	21.554	1.837	69.32
18	M3-300-15-1150-4-0	36.598	20.217	1.810	68.31
19	M3-300-60-1150-4-0	6.840	2.886	2.370	89.45
20	M3-500-15-1150-4-0	10.117	4.356	2.322	87.64
21	M3-500-60-1150-4-0	23.237	12.035	1.931	72.86
22	M1-0-0-1100-1-0	36.917	18.575	1.987	75.00
23	M1-0-0-1100-1-2	35.780	18.029	1.985	74.89
24	M1-0-0-1100-1-5	35.463	18.494	1.918	72.36
25	M1-0-0-1200-1-2	32.263	16.584	1.945	73.41
26	M1-0-0-1200-1-5	29.337	15.322	1.915	72.25
27	M1-0-0-1100-4-0	36.625	18.988	1.929	72.78
28	M1-0-0-1100-4-2	35.509	18.095	1.962	74.05
29	M1-0-0-1100-4-5	35.463	18.494	1.918	72.36
30	M3-0-0-1050-4-5	40.018	22.568	1.773	66.91
31	M3-0-0-1100-4-5	39.094	22.186	1.762	66.50
32	M3-0-0-1150-4-5	38.187	21.239	1.798	67.85
33	M3-300-60-1000-4-5	3.333	1.414	2.358	88.97
34	M3-300-60-1050-4-5	7.788	3.283	2.372	89.52
35	M3-300-60-1100-4-5	10.166	4.411	2.305	86.98
36	M3-300-60-1150-4-5	13.217	5.861	2.255	85.10